united nations educational, scientific and cultural organization

international atomic energy agency

the
abdus salam
international centre for theoretical physics

H4.SMR/1150 - 22

Fifth Workshop on Non-Linear Dynamics
and Earthquake Prediction

4 - 22 October 1999

Earthquake Occurrence

Antoni M. Correig

Departament d'Astonomia i Meteorologia
Universitat de Barcelona
Barcelona, Spain

EARTHQUAKE OCCURRENCE

Antoni M. Correig

Departament d'Astronomia i Meteorologia
Universitat de Barcelona

Marti Franques, 1. E-08028 Barcelona. Spain.
e-mail: anton@mizar.am.ub.es

INTRODUCTION

The Earth was formed as a planet of the Solar System about 4.5 billion years ago. Whether because of an initial high temperature, or due to radioactivity, the temperature distribution inside the Earth is slightly super-adiabatic, thus allowing for thermal convection at the outer core, which gives rise to the Earth's magnetic field, and convection at the mantle providing the mechanism for plate tectonics. Because the surface of the Earth is much colder temperature ($\sim 273K$) than the base of the mantle ($\sim 3000K$), the cold thermal boundary layer develops a few lithospheric plates, rigid layers with an average thickness of 0-80 km under the oceans and 150-200 km under the continents. The lower limit of the lithosphere is defined by an isotherm of $\sim 1600K$. The layers are in relative motion at a velocity of $2-10$ km/year, accumulating strain at their borders and thus generating stress. When the stress exceeds the resistance of the material a rupture occurs with a sudden release of energy, and with a consequent drop of the accumulated stress; this energy release, part of which propagates through the Earth as seismic waves, is known as an *earthquake*. However, tectonic plates continue to move, and the process is repeated. Thus a stationary state has been reached, consisting of deformation, stress accumulation and earthquake occurrence. This process is known as *seismic cycle*, and the interval of time elapsed between two consecutive earthquakes as *recurrence time*.

The various processes that constitute the seismic cycle occur at different time scales. The accumulation of stress caused by platae motions takes 100-1000 years (order of magnitude of $10^9 - 10^{10}$ s) and corresponds to the duration of the seismic cycle, and the release of energy is of the order of 1-2 minutes (order of magnitude of 10^2 s). Thus any model must take both these time scales into account, in addition to a third time scale, that of aftershocks, thatcan last for one year (order of magnitude of 10^7 s). We can thus say that eathquake occurrence is a complex process of stress relaxation characterized by three time scales, one of them much lower than the other two. Besides, during the seismic cycle, apart from the main shock, foreshocks and aftershocks, there also occur events of lower energy with an apparently random time and space distribution.

1 RECURRENCE OF EARTHQUAKES AND PROBABILISTIC PREDICTION

1.1 Earthquakes

As a result of the study of the 1906 San Francisco earthquake, Reid proposed a mechanism for the origin of earthquakes, known a *elastic rebound theory*, based on a loading process followed by a sudden energy release (Scholz, 1990), see Figure. According to Reid's model, an earthquake is just the rupture we have been talking about in the introduction, defined by its slip (a measure of the discontinuity across the fault plane), also known as dislocation.

From a mathematical point of view it is not convenient to deal with discontinuities (laws of physics are not valid there), and they are substituted by an equivalent system of forces: equivalent in the sense that a seismograph would record the same displacement field as that generated by the dislocation (see Aki and Richards, 1980, for a compl^te description). It has been found that the system of forces equivalent to a dislocation is a double couple with zero moment. The spatial orientation of the double couple is given in terms of two symmetric elements of a second-order symmetric tensor. Because we are considering only shear faults, the diagonal elements will vanish. Hence, all elements of the matrix $[A]$ associated to the tensor will be zero except for two symmetric elements, $a_{21} = a_{12} = 1$ for example. The strength of the double couple is given by the moment of either couple, known as *seismic moment* M (a scalar), and found to be the product of the medium rigidity, the area of the fault plane and the average dislocation. As a final result, the seismic source is represented by a second order symmetric tensor the matrix of which is given by $M[A]$. Because the trace of the matrix is zero, its determinant is zero, and hence has only four degrees of freedom: one degree for the norm M of the tensor and three degrees for the spatial orientation of the double couple, or, equivalently, the slip, which is known as *focal mechanism*. The focal mechanism can be retrieved from the direction of the first motion of the P-wave, and the seismic moment from its amplitude. These four parameters characterize the geometry and strength of the seismic source. However, we also need to know its spatial location (hypocenter) and the occurrence time. These four parameters are routinely determined from the arrival time of seismic waves at different seismic stations. In short, an individual earthquake is characterized by two sets of four parameters, on set consisting in the spacio-temporal location, and the other in the geometrical orientation of the source and its strength.

The strength of the earthquake is given in terms of the magnitude, a measure of the energy released by the earthquake and propagated as elastic waves, which is computed from the measurement of the maximum amplitude of a given part of the seismogram, approximately proportional to the logarithm of the seismic moment. It would be preferable to measure the earthquake's strength from the energy released, but this cannot be measured directly. It seems that the best solution consists in characterizing the earthquake strength through the (scalar) seismic moment.

1.2 Seismic cycle

Reid also observed, and this has been widely confirmed, that large earthquakes repeatedly occur on preexisting faults. Due to friction the fault is locked and accumulates strain at both sides until the tangential component of the stress exceeds the forces of friction leading the fault to rupture again. As the tectonic process can be considered as stationary, the accumulated stress will also be stationary, suggesting that earthquakes occur at preexisting faults at more or less regular intervals of time, known as *recurrence intervals*. Shimazaki and Nakada (1980) suggested a qualitative model for earthquake prediction based on the observed recurrence times, see Figure. Let T_1 represent the resistance of material to rupture, and T_2 the drop of stress after the rupture, which will depend on the local friction on both sides of the fault. If T_1 and T_2 are constant, the model will be predictable (periodic recurrence times) and with constant slip (all earthquakes with the same magnitude). This similarity of each earthquake originates the concept of *characteristic earthquake*, according to which faults are segmented, and the distinct individual segments behave in a predictable way.

Unfortunately, the periodic recurrence time has not been observed, and two variations of the predictive model were proposed by Shimazaki and Nakada, the *time predictable* model and the *slip predictable* model. In the time predictable model T_1 is constant and T_2 is variable, see Figure; the occurrence time of the next earthquake is obtained from the observed slip of the last one. In the slip predictable model T_1 is variable and T_2 is kept constant: the slip of the next earthquake can be predicted on the basis of the time elapsed since the previous earthquake. However, comparing both models with observations (instrumental, historical and paleoseismic data) we can see that the mean recurrence time is well defined, but with significant and unpredictable fluctuations. In other words, no deterministic prediction is possible.

Fortunately, however, not everything is lost. In the first place, the total slip across a fault has to balance plate motions: if a fault is segmented the total slip of the distinct segments, averaged over several seismic cycles, has to be consistent with the expected slip. In the second place, the processes that drive plate tectonics are approximately stationary, thus allowing, in principle, an estimation of the mean recurrence time. In the third place, we have seen that the active faults are segmented and each earthquake occurs in a given segment. If the seismic history of a seismic fault is known for a period of time longer than the recurrence time, it is possible to detect whether a segment remains intact. This unbroken segment is known as *seismic gap*. If a seismic gap is detected, it can be attributed high potential hazard.

1.3 The recurrence of earthquakes as a nonlinear system

It has been widely observed that the recurrence time of earthquake occurrence is not periodic; in other words, we cannot predict deterministically the occurrence of the next earthquake from the observations of a few past earthquakes. Much has been studied in physics about nonlinear dynamical systems, although their application to seismology is still scarce. There is a model that, at first sight, fits our needs, the *dripping faucet* (Shaw, 1984). From an experimental point of view, water from a tank is measured as it passes through an adjustable brass nozzle. Depending on the flow rate of water, the drop rate can be periodic, quasi-periodic or chaotic. Upon substitution of the word *water* by the word *stress*, the analogy between recurrence of earthquakes and recurrence of drops is total. To simulate the dripping faucet Shaw (1984) designed a very simple mathematical model: a mass, representing the drop, grows linearly in time, stretching a spring that represents the force of surface tension. When the spring reaches a certain length the mass is suddenly reduced, representing a drop detaching, by an amount dependent on the speed of the mass when it reaches the critical distance. We thus have driven nonlinear oscillator, the nonlinearity arising from the sudden change in mass, and with position, velocity and mass providing the three variables required for the occurrence of chaotic behavior in a system evolving in continuous time. Numerical simulations show that the dripping faucet model is able to reproduce the main features of the (few) observed recurrence time of earthquakes.

1.4 A probabilistic approach to recurrence time prediction

The goal of any model is to predict future events. A generalization of Reid's model led to Shimizaki and Nakada's time-predictable and slip-predictable deterministic models. Under the hypothesis (Hagiwara, 1974) that the statistical distribution of the ultimate crust strain may be represented by a Weibull distribution, Rikitake (1975, 1999) estimated the probability of occurrence of great earthquakes . We have tested Hagiwara-Rikitake's approach with data generated by the dripping faucet model in the chaotic regime and found that the estimated recurrence time with its associated standard deviation was kept almos constant through the evolution of a window of 15 points for a generated time series of 2,000 elements.

2 THE PHYSICAL BASES OF THE SEISMIC CYCLE

2.1 Phenomenology of seismic catalogs and fault population

Up to now we have characterized the seismic cycle by the main shock. However, a look at any seismic catalog reveals the occurrence of other events apart from the characteristic ones.

As reported by Main (1996), an analysis of the seismic catalogs and fault population reveals the following characteristics:

1. Fault populations are broadly scale-invariant over several orders of magnitude (power law distribution).

2. Earthquake frequency-magnitude statistics also imply power law scaling (Gutenberg-Richter law).

3. Earthquakes have a relatively constant and relatively small stress drop over a wide range of scales during dynamic slip (3 MPa compared with tectonic stress, $\sim 10 - 100$ Mpa .

4. Fault and fracture breaks are rough, with self-affine or self-similar scaling.

5. Earthquake population in diverse tectonic zones exhibit spatial variability, clustering and intermittency, quantitatively consistent with multifractal scaling.

6. The distribution of spacings of hypocentral locations of earthquakes and laboratory acoustic emissions are power law in both space and time.

7. Earthquakes have aftershock sequences that decay at a rate $R(t)$ determined by Omori's law $R(t) = \frac{R_0}{(t+t_0)^p}$, where p is a power law index and R_0 and t_0 are constants.

8. Seismicity can be induced by stress perturbations smaller than the stress drop in individual events; i.e., earthquakes can be "triggered".

In short, we can say that the seismic catalog is characterized by a clustering in the seismic cycle (foreshocks, main shock, aftershocks), power law distributions (Gutenberg-Richter's law, Omori's law), fractal and multifractal scaling and action at distance. From a phenomenological point of view, these are the characteristics of a fractal structure. Following Ito (1992), we can say that **earthquakes are natural fractals**. We are thus left to find the physical process according to which the occurrence of earthquakes emerges as a fractal structure, as many other natural phenomena.

The best known scale free phenomena in physics are the critical phenomena that occur at the phase transitions. Well known phase transitions are liquid-gas transition at the critical temperature and the magnetic transition ferromagnetic-paramagnetic. In general terms we can view a phase transition as a transition order-disorder: in the liquid-gas transition, liquid is in an ordered state, and gas in a disordered; in the magnetic transition, below the critical temperature the material is in an ordered state (dipoles are in the same direction), and above the critical temperature in a disordered state (dipoles lie on a random direction). An earthquake is a large-scale fracture of the earth's crust, with a sudden release of stored energy, and it occurs when the stored energy exceeds the resistance of the material. The critical point will thus be defined as the resistance of material to failure. The ordered state will correspond to the stressed material, and the disordered state to the unstressed material (note that although we are dealing with stress as a scalar, it is a tensor!).

Take again the example of the liquid-gas phase transition. For a given range of pressure and temperature, liquid and gas coexist, with a step in density; as the critical point is approached the density step decreases, vanishing at the critical point. For temperature higher than the critical one, liquid and gas cease to be distinct entities. It is interesting to note that, as we approach the critical point *critical opalescence* appears: close to the critical point long-range fluctuations appear in the density of the fluid. If light is shone on to a fluid near its critical temperature it is strongly reflected and causes the fluid to appear milky-white, due to the existence of fluctuations at all scale lengths, obeying a power law distribution. It thus appears that the liquid-gas phase transition can be defined by two parameters: the density step of the phase transition and the length-scale of the fluctuations. Both parameters define the evolution of all classes of critical phenomena, and are generically termed **order parameter** and **correlation length**.

The order parameter $\phi(x,t)$ accounts for the temporal and spatial evolution of some defined parameter along the line that separates two phases: clearly, at the critical point the order parameter vanishes. In the liquid-gas transition the order parameter is defined as $\phi(x) = \rho(x) - \rho_{gas}(x)$. There is no general scheme for defining order parameters: one has to consider each new physical parameter afresh. In the case of an earthquake, it occurs when the stored energy exceeds the frictional stress $\sigma_{fr}(x)$, so we can define the order parameter as $\phi(x) = \sigma(x) - \sigma_{fr}(x)$; because of the inhomogeneities of the fault, we will have different values along it. Note that we can also define the order parameter in terms of the slip $u(x)$ on the fault, which is proportional to the stress drop, which in turn is related to the accumulated stress. Also note that the order parameter vanishes as the critical point is reached.

The correlation length ξ expresses the typical distance over which the behavior of a variable is correlated with, or influenced by, the behavior of another variable, and can be viewed as a measure of the typical linear dimension of the largest piece of correlated spatial structure. The correlation length is related to the spatial fluctuations of the order parameter. It has been found empirically that the correlation length is proportional to $\xi \sim\mid p-p_c \mid^{\nu}$, where p is the parameter that defines the phase transition and p_c its critical value (that is, temperature, pressure, stored stress in the above examples.) Clearly, at the critical point ξ diverges and all scale lengths are present, and follow a power law distribution. This divergence of the correlation length is a necessary condition for the *action at distance*. In the case of earthquakes, the correlation length can be associated with the length of the fault.

In summary, the theory of critical phenomena is able to account for all phenomenological characteristics of the seismic catalogs, *i.e.*, selfsimilarity (power law behavior) and action at distance. Care has to be taken, however, in remembering that the critical opalescence (fluctuations at all scale lengths), the equivalent to the occurrence of foreshocks, main shock and aftershocks, occurs only close to the critical point.

2.2 Self organized critical models

The theory of critical phenomena is able to explain the phenomenology of earthquake catalogs. On the other hand, they are referred to laboratory conditions: one or more parameters need to be tuned to reach the critical point (for example, pressure and temperature in liquid-gas transition). This fact also implies that critical phenomena are not time dependent and, as a consequence, do not display any characteristic time scale. This aspect disagrees with observations, characterized by two time scales (three if after shocks are allowed to), one related to the loading process and the other to the rupture time. We can define a tuning parameter as the stress loading, a function of the plate velocity. Any physical model for earthquake occurrence, thus, has to incorporate this characteristic time scale, as well as the time scale of rupture which will occur when a critical point is reached. Basically two such models have been proposed, with multitude of variations: the slider-block model and the sand-pile model. Further, it has been shown that, under very general conditions, a mapping can be defined from one of them to the other, revealing that they represent different aspects of the same phenomenon.

2.2.1 Slider-block model

As a working hypothesis, widely accepted nowadays, we assume that earthquakes occur repeatedly on preexisting faults. Burridge and Knopoff (1967) constructed a slider-block model to simulate the stick-slip rupture on a fault. The model consists of two (tectonic) plates that sandwich a chain of N blocks (later on extended to a bidimensional network of $N \times N$ blocks) of equal mass m, mutually coupled by springs of Hooke constant k_c and equilibrium length a. The blocks are pulled by the bulk of one plate moving at velocity V through constant elastic shear k_p against the friction F_p between the two plates. The friction prevents sliding of the blocks until a critical value of the pulling force is reached. The block sticks and the force on the spring increases until it equals the friction resistance to sliding on the surface, and then slip occurs. The extension of the spring is analogous to the elastic strain in the rock adjacent to a fault. The slip is analogous to an earthquake on a fault. When the slip occurs, the stored elastic strain in the spring is relieved and this process corresponds to the elastic rebound on a fault. In the stationary state, the equation of motion for the ith block is

$$m\ddot{X} = k_c(X_{i+1} - 2X_i + X_{i-1}) - k_p(X_i - Vt) - F_p(\dot{X}_i)$$

where X_i is the departure of block i from its equilibrium position.

This set of coupled differential equations has to be solved numerically for the whole system simultaneously, and is very time consuming. An extension to two dimensions with an analog cellular automaton was designed by Nakanishi (1990), much faster in computation. The blocks interact with their nearest neighbors, so in any step in a loop one has to consider the possible slip of any of the blocks of the system. If we define the *size of the earthquake* as the number of blocks that have slid, the size distribution follows a power law, thus satisfying Gutenberg-Richter law. However, no aftershocks are allowed in this model: all events are independent, corresponding to independent steps in the loop. On the other hand, this is the condition of applicability of Gutenber-Richter law: to be computed, foreshocks and aftershocks have to be removed from the seismic catalog. To generate aftershocks, the hypothesis of viscoelasticity has to be introduced. In the slider block model, two different time scales are present: a very large one, related to the plate motion, and a short one (considered as instantaneous)corresponding to the total slip of the system.

It is of interest to point out some features of the slider-block model: for high dimensional systems (a large number of blocks) the system behaves at the edge of chaos, and for low dimensional systems (a few blocks, often used to simulate the interaction between faults), the system is chaotic. Thus, the prediction of individual earthquakes is not possible in a deterministic sense, and only a probabilistic approach will be possible.

2.2.2 Sand-pile model

Consider a pile of sand on a circular table (Bak *et.al.*, 1988, Turcotte, 1997). Grains of sand are randomly dropped on the pile until the slope of the pile reaches the critical angle of repose. This is the maximum slope that granular material can maintain without additional grains sliding down the slope. The sand-pile never reaches the hypothetical critical state. As the critical state is approached additional sand grains trigger sandslides of various sizes, and the frequency-size distribution of landslides is a power law. On average the number of sandgrains added balance the number that slide down the slope and off the table, but the actual number of grains on the table fluctuates continuously. The evolution of the above system is well illustrated using a simple cellular automata model (Vespignani and Zapperi, 1998). Consider a squared grid of N boxes, and let z_i be an integer (or continuous) variable that represents the number of grains (energy) that we add to the system. At each time step an energy grain is added to a randomly chosen site, until the energy of a site reaches a threshold z_c. When this happens the site relaxes

$$z_i \longrightarrow z_i - z_c$$

and the energy is transferred to the nearest neighbors

$$z_j \longrightarrow z_j + y_i.$$

The relaxation of a site can induce nearest neighbor sites to relax on their turn, *i.e.*, they exceed the threshold because of the energy received. New active sites can generate other relaxations and so on, eventually giving rise to an avalanche. The distribution of avalanches follows a power law distribution. As already noted, under very general conditions we can assimilate the relaxation of a grain to the sliding of a block in the spring-block model, which can be described by a cellular automaton model similar to the one just described.

2.3 Self-Organized Criticality

The two models previously described are typical examples of large interactive systems. To describe their behavior, Bak *et.al.* (1988) introduced the concept of Self-Organized Criticality (SOC). A system is said to be in a state of Self-Organized Criticality if it is maintained near a critical point. According to this concept a natural system is in a marginally stable state; when perturbed from this state, it will evolve naturally back to the state of marginal stability. In the critical state there is no longer a natural length scale, so that fractal statistics applies.

The SOC model solves, for example, the problem of the external tuning for the system to reach the critical point, but is very sensitive to other parameters such us the velocity of the driving plates. Perhaps it is too simplistic, but has helped us to understand the general features of earthquake occurrence as a complex system, which is composed of a very large number of elements and initiated the point of view of assimilate the occurrence of earthquakes to critical phenomena.

Vespignani and Zapperi (1988) have shown that the number of states needed to describe each site can be reduced to the following three main states: stable, critical and active. *Stable* sites are those that do not relax (become active) if energy is added to them by external fields or interactions with active sites. *Critical* sites become active with the addition of energy. *Active* sites are those transferring energy; they interact with other sites, usually nearest neighbors.

Correig *et.al.* (1997) provide an example of a three state system, the so called *minimalist model*.

REFERENCES

Aki, K. and Richards, P.G. (1980). *Quantitative seismology*, Freeman.

Bak, P., Tang, C. and Wiesenfeld, K. (1988). Self-Organized criticality, *Phys. Rev. A*, **38**, 364-374.

Burrigde, R. and Knopoff, L. (1967), Model and theoretical seismology, *Bull. Seism. Soc. Am.*, **57**, 341-371.

Correig, A.M., Urquizu, M., Vila, J. and Manrubia, S. (1997). Aftershock series of event February 18, 1996: An interpretation in terms of self-organized criticality, *J. Geophys. Res.*, **B102**, 27,407-20.

Hagiwara, Y. (1974). Probability of earthquake occurrence as obtained from a Weibull distribution analysis of crustal strain, *Tectonophysics*, **23**, 313-318.

Ito, K. (1992). Towards a new view of earthquake phenomena, *Pure appl. Geophys.*, **138**, 531-548.

Main, I.)1996). Statistical physics, seismogenesis and seismic hazard, *Rev, Geophys.*, **34**, 433-462.

Nakanishi, H. (1990). Cellular automaton model of earthquakes with deterministic dynamics, *Phys. Rev. A*, **41**, 7086-7089.

Rikitake, T. (1975). Statistics of ultimate strain of the earth's crust and probability of earthquake occurrence, *Tectonophysics*, **26**, 1-21.

Rikitake, T. (1999). Probability of a great earthquake to recur in the Tokai district, Japan: reevaluation based on newly-developed paleoseismology, plate tectonics, tsunami study, microseismicity and geodetic measurements, *Earth, Planets, Space*, **51**, 147-157.

Scholz, C.H. (1990). *The mechanics of earthquakes and faulting*, Cambridge.

Shaw, R. (1984). *The dripping faucet as a model chaotic system*, Aerial Press, Santa Cruz, CA.

Shimazaki, K. and Nakada, T. (1980). Time predictable recurrence model for large earthquakes, *Geophys. Res. Lett.*, **7**, 2679-2682.

Turcotte, D.L. (1997). *Fractals and chaos in Geology and Geophysics*, Cambridge.

Vespignani, A. and Zapperi, S. (1998). How self-organized criticality works: a unified mean-field picture, *Phys. Rev. E*, **57**, 6345-6362.

GENERAL BIBLIOGRAPHY

Jensen, H.J. (1998). *Self-Organized Criticality*, Cambridge.

Lay, T. and Wallace, T.C. (1995). *Modern global seismology*, Academic Press.

Turcotte, D.L. (1997). *Fractals and chaos in Geology and Geophysics*, Cambridge.

Turcott, D.L. and Schuber, C. (1982). *Geodynamics*, John Wiley.

Wyss, M., Shimazaki, K. and Ito, A., Eds. (1999). Seismicity patterns, their statistical significance and physical meaning, *Pure appl. Geophys.*, **155** (special issue).

Yeomans, J.M. (1997). *Statistical mechanics of phase transitions*, Oxford.

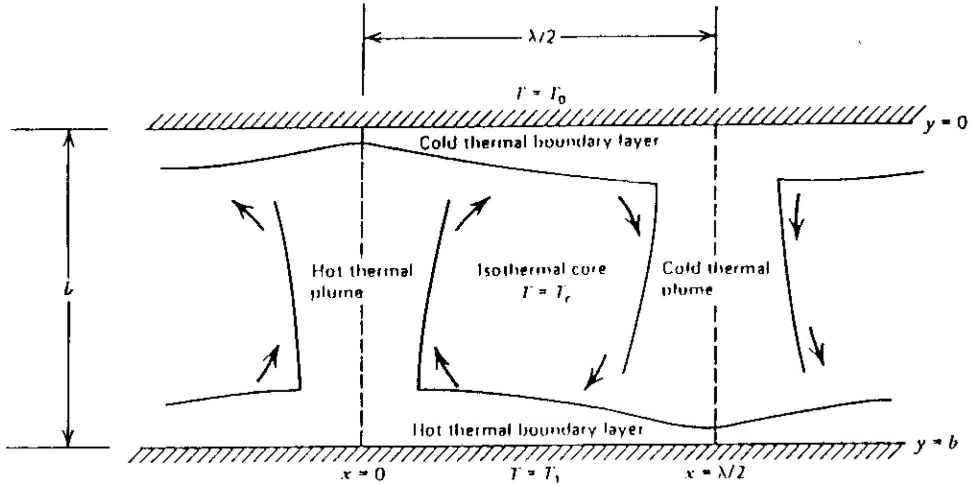

Figure 6-39 Boundary layer structure of two-dimensional thermal convection cells in a fluid layer heated from below.

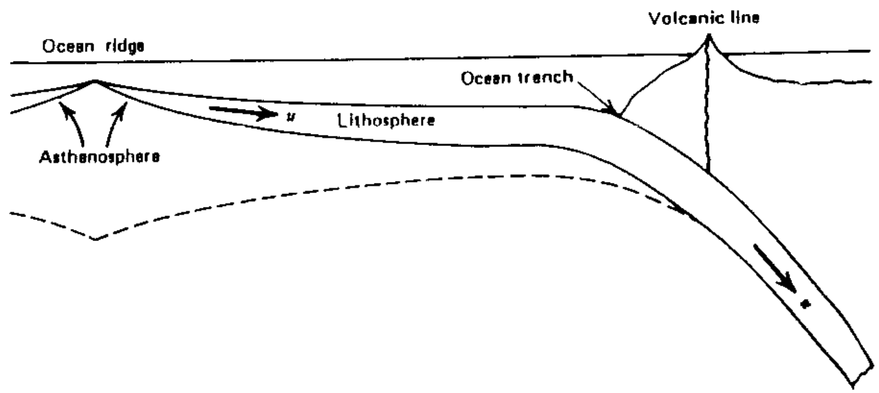

Figure 1-2 Accretion of a lithospheric plate at an ocean ridge and its subduction at an ocean trench. The asthenosphere, which lies beneath the lithosphere, is shown.

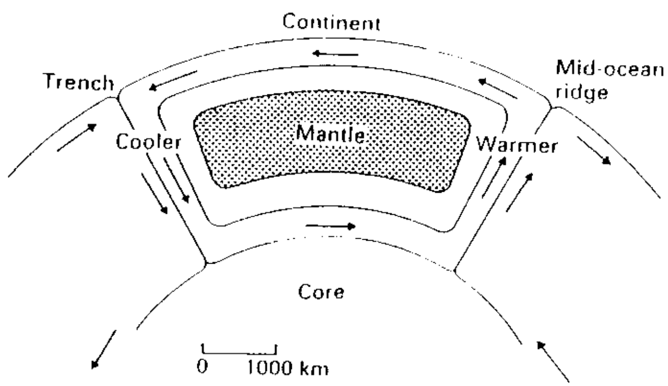

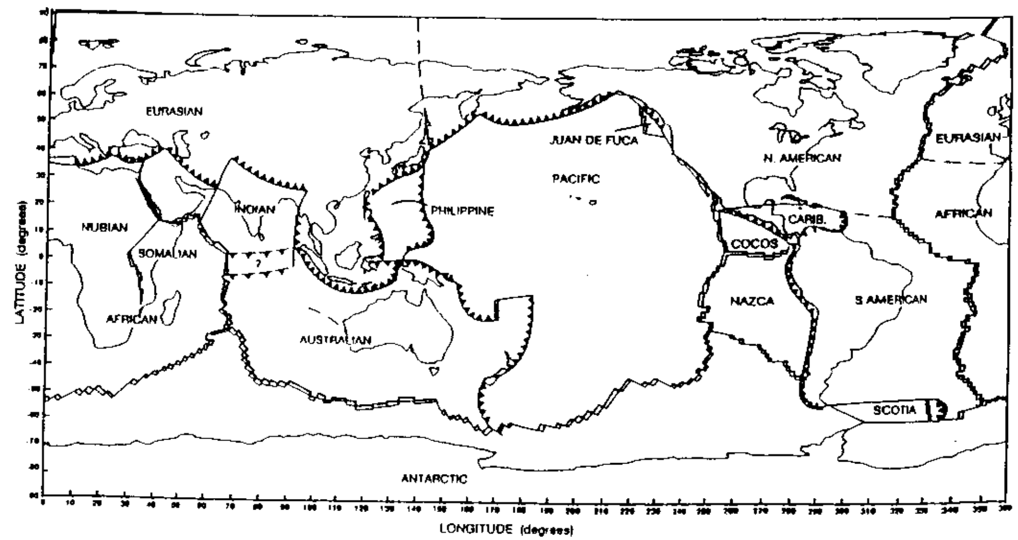

Figure 4.2. The Earth's major plates. Subduction zones are represented by "sharks' teeth" drawn on the over-riding plates and showing the motion of the subducting plates beneath. Spreading centres are marked by double lines, but they are fragmented by transform faults (single lines as in Fig. 4.18). Broken lines mark uncertain boundaries.

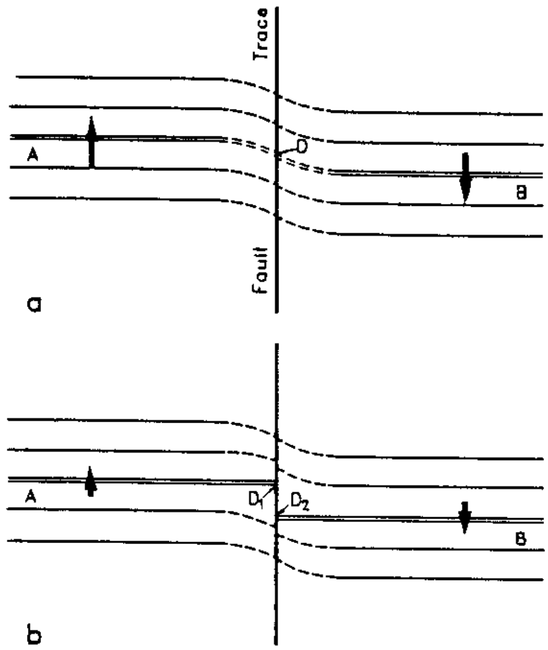

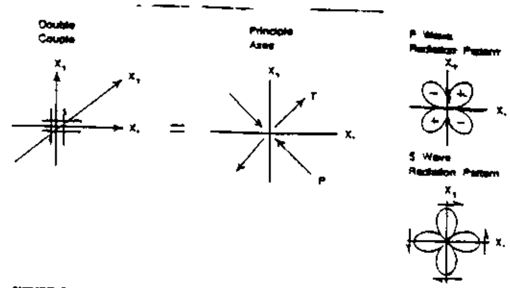

FIGURE 6.10 The double-couple force system in the x_1x_3 plane for a shear dislocation in the x_1x_2 plane. An equivalent set of point forces composed of two dipoles without shear on the principal axes, is shown in the center. On the right are the patterns of P- and S-wave radiation distributed over the respective wavefronts in the x_1x_2 plane.

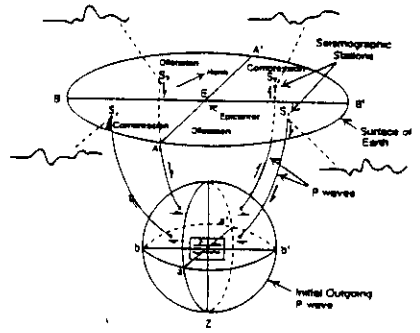

FIGURE 6.8 First motions of P waves at seismometers located in various directions about an earthquake allow determination of the fault orientation. P waves, for which upward motions are compressional (away from the source) and downward motions are dilatational (toward the source), exhibit a simple alternation with quadrants for a vertical strike-slip fault, as shown. (Modified from Bolt, 1988. Copyright © 1988 by W. H. Freeman and Co. Reprinted with permission.)

3.3 General Analysis of Displacement Discontinuities Across an Internal Surface Σ

In this section we shall introduce the seismic *moment tensor*, M. This is a quantity that depends on source strength and fault orientation, and it characterizes all the information about the source that can be learned from observing waves whose wavelengths are much longer than the linear dimensions of Σ. In this case, the source is effectively a point source with an associated radiation pattern, and the moment tensor can often be estimated in practice for a given earthquake by using long-period teleseismic data. In practice, seismologists use moment tensors that are confined to sources having a body-force equivalent given by couples alone. Such sources include geologic faults (shearing) and explosions (expansion), with M as a second-order tensor. For forces differentiated more than once, sources can be characterized by higher-order moment tensors.

For sources of finite extent, we shall introduce the seismic *moment density tensor*, m, which can often be thought of as $d\mathbf{M}/d\Sigma$, or as $d\mathbf{M}/dV$ for a volume source.

There are two ways in which this section generalizes Section 3.2. First, the coordinate axes are not taken in directions related to directionalities of the source. (This generality is important, because the direction of slip and the orientation of the fault plane are not usually known *a priori*, but must be deduced from the radiated seismic waves.) Second, discontinuities are to be allowed in the displacement component normal to the fault plane, so that apparent expansions or compressions will be allowed to occur.

Our starting point for the general analysis of displacement discontinuities is the representation (3.2), but using now the convolution symbol $*$ so that

$$u_n(\mathbf{x}, t) = \iint_\Sigma [u_i]\nu_j c_{ijpq} * \frac{\partial}{\partial \xi_q} G_{np}\, d\Sigma. \tag{3.17}$$

If X_0 is the amplitude of a force applied in the p-direction at ξ with general time variation, then the convolution $X_0 * G_{np}$ gives the n-component of displacement at $(\mathbf{x}, t)$ due to the varying point force at ξ. More generally, if the force applied at ξ is $\mathbf{F}(\xi, \tau)$, then we can sum over p and write $F_p * G_{np}$ for the n-component

$[u_i]\nu_j c_{ijpq}$ are moment per unit area, and this makes sense because the contribution from ξ has to be a surface density, weighted by the infinitesimal area element $d\Sigma$ to give a moment contribution. We define

$$m_{pq} \equiv [u_i]\nu_j c_{ijpq} \tag{3.18}$$

to be the components of the *moment density tensor*, m. In terms of this symmetric tensor, which is time dependent, the representation theorem for displacement at x due to general displacement discontinuity $[\mathbf{u}(\xi, \tau)]$ across Σ is

$$u_n(\mathbf{x}, t) = \iint_\Sigma m_{pq} * G_{np,q}\, d\Sigma. \tag{3.19}$$

When we have learned more about the Green function (in Chapter 4), we shall find that the time dependence of the integrand in (3.19) is quite simple, because if x is many wavelengths away from ξ, then convolution with G gives a field at $(\mathbf{x}, t)$ that depends on what occurs at ξ only at "retarded time," i.e., t minus some propagation time between ξ and x.

For an isotropic body, it follows from (2.33) and (3.18) that

$$m_{pq} = \lambda\nu_k[u_k(\xi, \tau)]\delta_{pq} + \mu(\nu_p[u_q(\xi, \tau)] + \nu_q[u_p(\xi, \tau)]). \tag{3.20}$$

Further, if the displacement discontinuity (or slip) is parallel to Σ at ξ, the scalar product $\nu \cdot [\mathbf{u}]$ is zero and

$$m_{pq} = \mu(\nu_p[u_q] + \nu_q[u_p]). \tag{3.21}$$

In the case of Σ lying in the plane $\xi_3 = 0$, with slip only in the ξ_1-direction, we have the source model considered in Section 3.2, and for this the moment density tensor is

$$\mathbf{m} = \begin{pmatrix} 0 & 0 & \mu[u_1(\xi, \tau)] \\ 0 & 0 & 0 \\ \mu[u_1(\xi, \tau)] & 0 & 0 \end{pmatrix},$$

which is the now familiar double couple.

In the case of a tension crack in the $\xi_3 = 0$ plane, only the slip component $[u_3]$ is nonzero, and from (3.20) we find

$$\mathbf{m} = \begin{pmatrix} \lambda[u_3(\xi, \tau)] & 0 & 0 \\ 0 & \lambda[u_3(\xi, \tau)] & 0 \\ \end{pmatrix}.$$

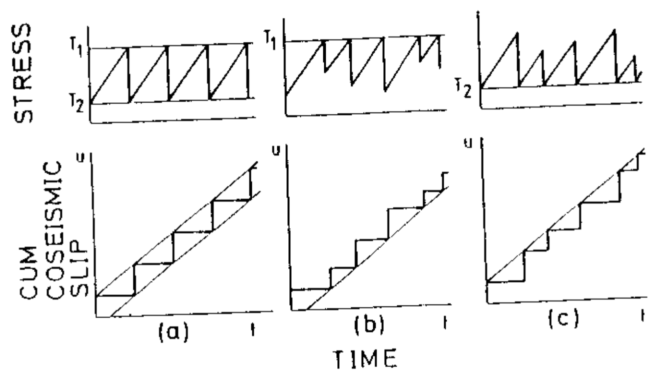

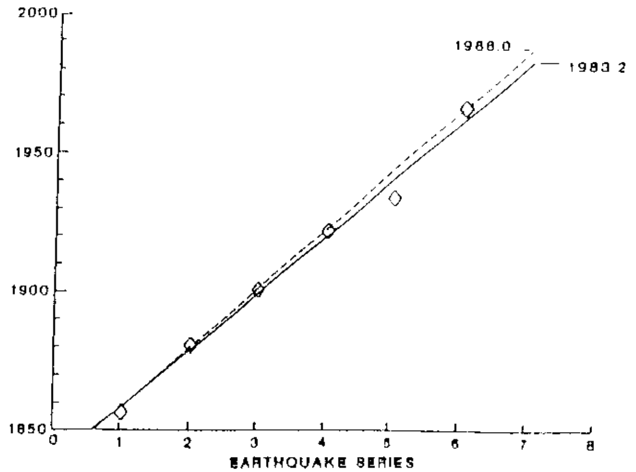

History of **Parkfield earthquakes**. Dashed line is a linear fit without the 1934 earthquake, solid line includes it. (From Bakun and McEvilly, 1984.)

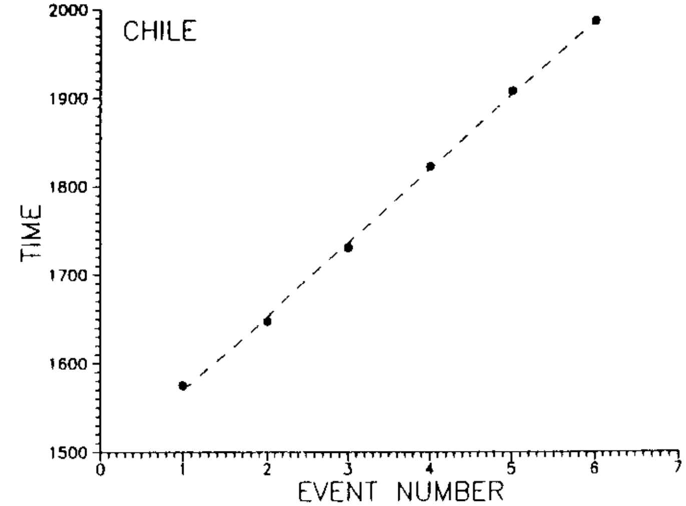

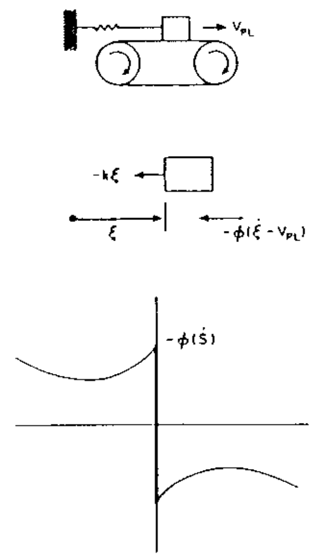

A simple mass–spring–slider model of earthquake recurrence: From the top, a schematic of the system – the mass rides on a conveyor belt and is restrained by the spring; the forces in the system and a

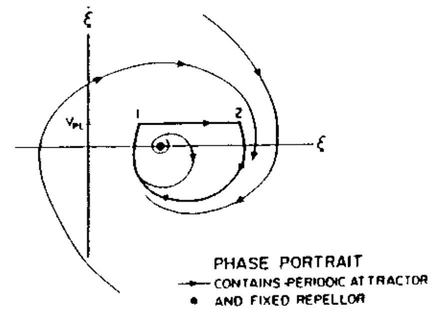

Phase portrait of the dynamic system. Thick orbit is a periodic attractor, closed circle a fixed repellor.

$$m\ddot{\xi} + \phi(\dot{\xi} - v_{pl}) + k\xi = 0$$

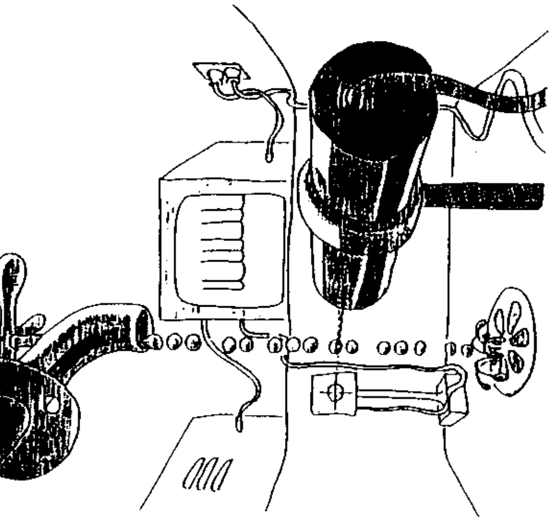

The apparatus.
(drawn by Chris Shaw)

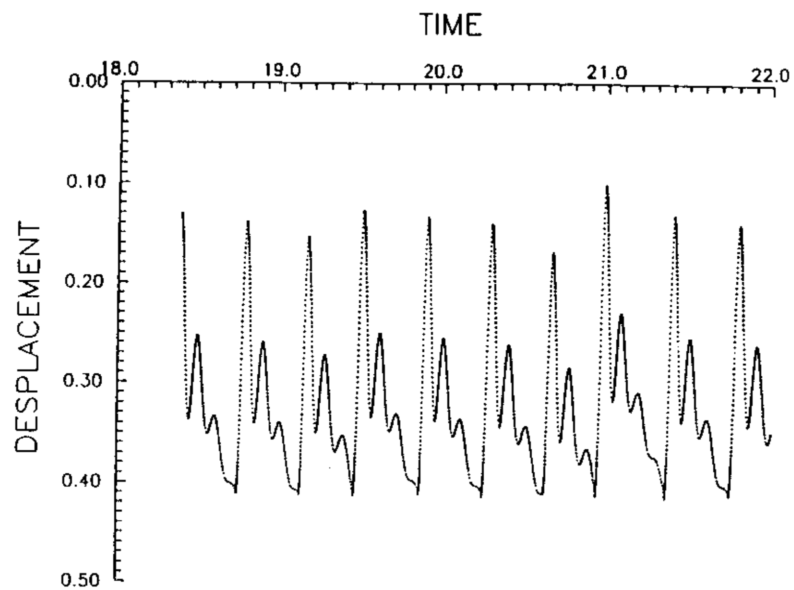

$$F = ma$$
$$mg - kx \approx m\ddot{x}$$
$$\dot{m} = \text{const.}$$
$$\Delta m \prec \dot{x}\Big|_{x=x_0}$$

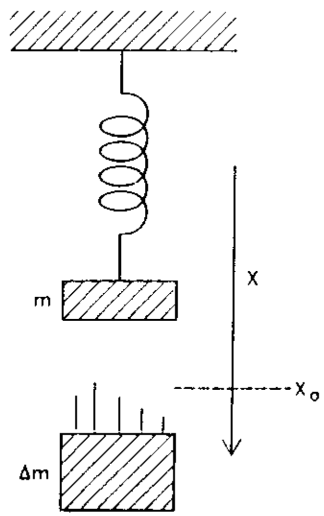

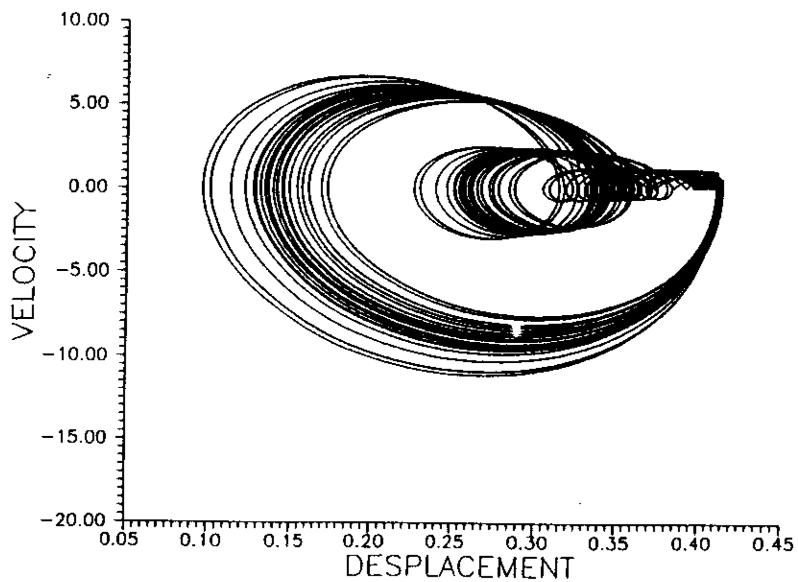

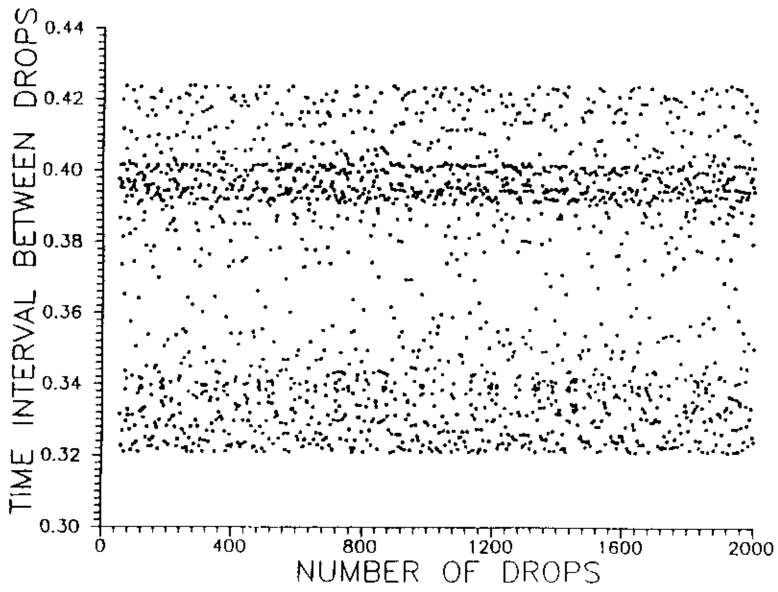
TIME INTERVAL BETWEEN DROPS
NUMBER OF DROPS
0.44
0.42
0.40
0.38
0.36
0.34
0.32
0.30
0
400
800
1200
1600
2000

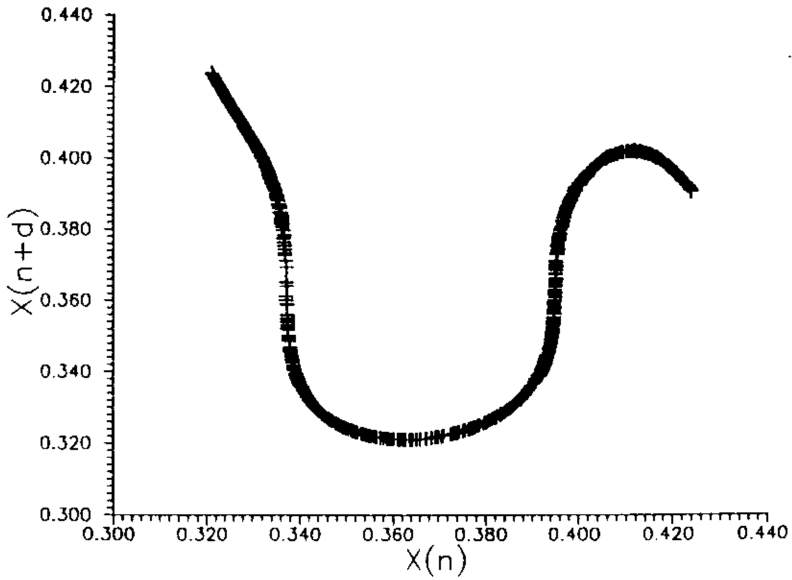
X(n+d)
X(n)
0.440
0.420
0.400
0.380
0.360
0.340
0.320
0.300

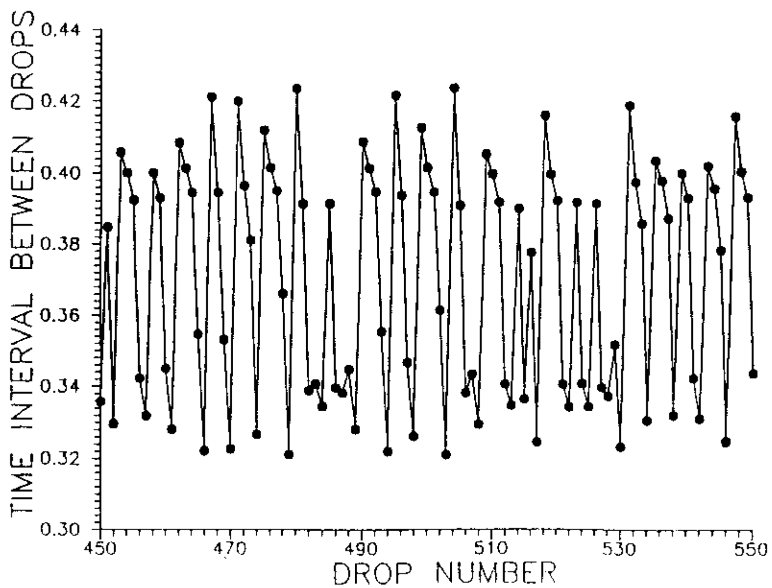
TIME INTERVAL BETWEEN DROPS
DROP NUMBER
0.44
0.42
0.40
0.38
0.36
0.34
0.32
0.30
450
470
490
510
530
550

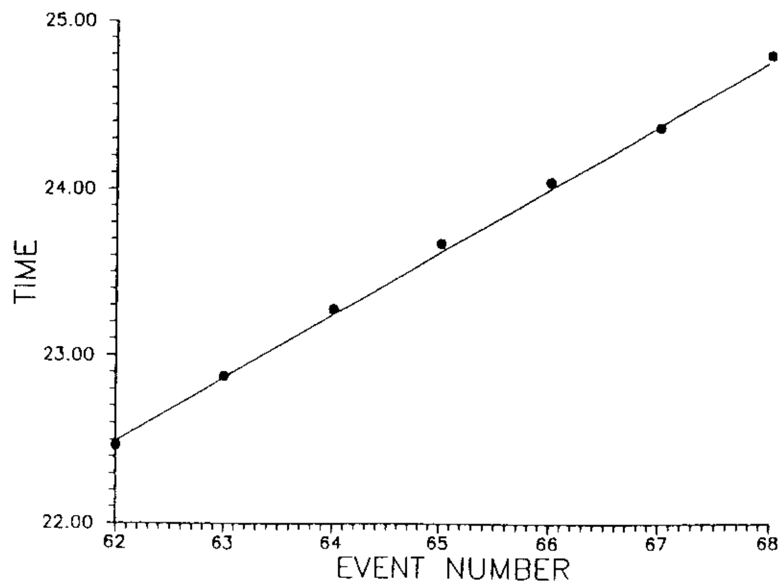
TIME
EVENT NUMBER
25.00
24.00
23.00
22.00
62
63
64
65
66
67
68

Weibull distribution analysis

The assumption that $\epsilon - E$ is governed by a Gaussian distribution is obviously inadequate because ϵ is to be defined over a range for which $\epsilon < 0$. In order to improve this point, Hagiwara (1974b) proposed to apply a Weibull distribution (Weibull, 1951), which has been widely used in quality control research, to the present analysis of probability. It has been proved that the distribution is very useful for analyses of the failure time of buildings, factory products and so on.

Let us denote a small time interval by Δt. The probability for crustal rupture to occur between t and $t + \Delta t$ is given by $\lambda(t)\Delta t$ on the condition that the rupture did not occur prior to t. $\lambda(t)$, called the hazard rate, is distributed in a Weibull distribution as:

$$\lambda(t) = Kt^m \qquad [15\text{-}30]$$

where $K > 0$ and $m > -1$.

The cumulative failure rate is given as:

$$F(t) = 1 - R(t) \qquad [15\text{-}31]$$

where $R(t)$ is called the reliability and defined by:

$$R(t) = \exp\left[-\int_0^t \lambda(t)\mathrm{d}t\right] = \exp\left(-\frac{Kt^{m+1}}{m+1}\right) \qquad [15\text{-}32]$$

Failure density function $f(t)$ is then obtained as:

$$f(t) = -\frac{\mathrm{d}R(t)}{\mathrm{d}t} = Kt^m \exp\left(-\frac{Kt^{m+1}}{m+1}\right) \qquad [15\text{-}33]$$

The mean time to rupture, or mean life so called in quality control research, is given as:

$$E[t] = \int_0^\infty t f(t)\mathrm{d}t = \left(\frac{K}{m+1}\right)^{-1/(m+1)} \Gamma\left(\frac{m+2}{m+1}\right) \qquad [15\text{-}34]$$

where Γ denotes a gamma function. In a similar fashion, the mean square of the time to rupture is obtained as:

$$E[t^2] = \int_0^\infty t^2 f(t)\mathrm{d}t = \left(\frac{K}{m+1}\right)^{-2/(m+1)} \Gamma\left(\frac{m+3}{m+1}\right) \qquad [15\text{-}35]$$

The standard deviation of the rupture time is defined by $(E[t^2] - E^2[t])^{1/2}$ which is obtained as:

$$(E[t^2] - E^2[t])^{1/2} = E[t]\left[\Gamma\left(\frac{m+3}{m+1}\right) - \Gamma^2\left(\frac{m+2}{m+1}\right)\right]^{1/2} \Big/ \Gamma\left(\frac{m+2}{m+1}\right) \qquad [15\text{-}36]$$

When the double logarithm of $1/R$ is taken, we obtain:

$$\log_e \log_e \left(\frac{1}{R}\right) = \log_e \left(\frac{K}{m+1}\right) + (m+1)\log_e t \qquad [15\text{-}37]$$

The above discussion has been developed in terms of t. It may be approximately assumed, however, that strain accumulation due to a plate motion proceeds with a constant strain rate u. The time origin is taken at the occurrence time of a large earthquake when most of the strain energy accumulated is released. In that case, we assume:

$$\epsilon = ut \qquad [15\text{-}38]$$

and so the entire discussion above can be made in terms of ϵ. For instance, [15-37] can be rewritten as:

$$\log_e \log_e \left(\frac{1}{R(\epsilon)}\right) = \log_e \left(\frac{Ku^{-m-1}}{m+1}\right) + (m+1)\log_e \epsilon \qquad [15\text{-}39]$$

which indicates that $\log_e \log_e (1/R)$ is linearly correlated with $\log_e \epsilon$.

In order to determine m and K from actual data, we usually proceed in the following way. Counting frequency of earthquake occurrence n_i for each strain range having an interval $\Delta\epsilon$, probability density for a range between $i\Delta\epsilon$ and $(i+1)\Delta\epsilon$ $(i = 0, 1, 2, \ldots)$ can be obtained from:

$$f_i \Delta\epsilon = n_i/N \qquad [15\text{-}40]$$

where N is the total number of the data. Accordingly, the cumulative probability is obtained as:

$$F = \Delta\epsilon \sum_{i=0}^{i} f_i = \sum_{i=0}^{i} n_i/N \qquad [15\text{-}41]$$

so that R can readily be calculated from [15-31].

The above-mentioned procedure is applied to the data of ultimate strain which are given in Table 15-XII. Omitting extreme values of ultimate strain such as those for the 1906 San Francisco, 1928 South Bulgaria and the 1933

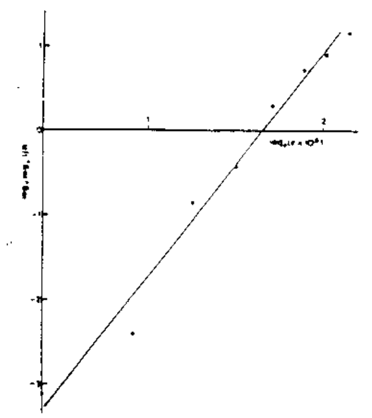

Fig. 9. $\log_e \log_e 1/R$ vs. $\log_e \epsilon$ fit for a Weibull distribution analysis of the whole set of data of ultimate strains.

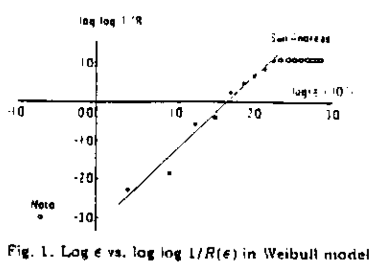

Fig. 1. Log ϵ vs. log log $1/R(\epsilon)$ in Weibull model curve-fitting.

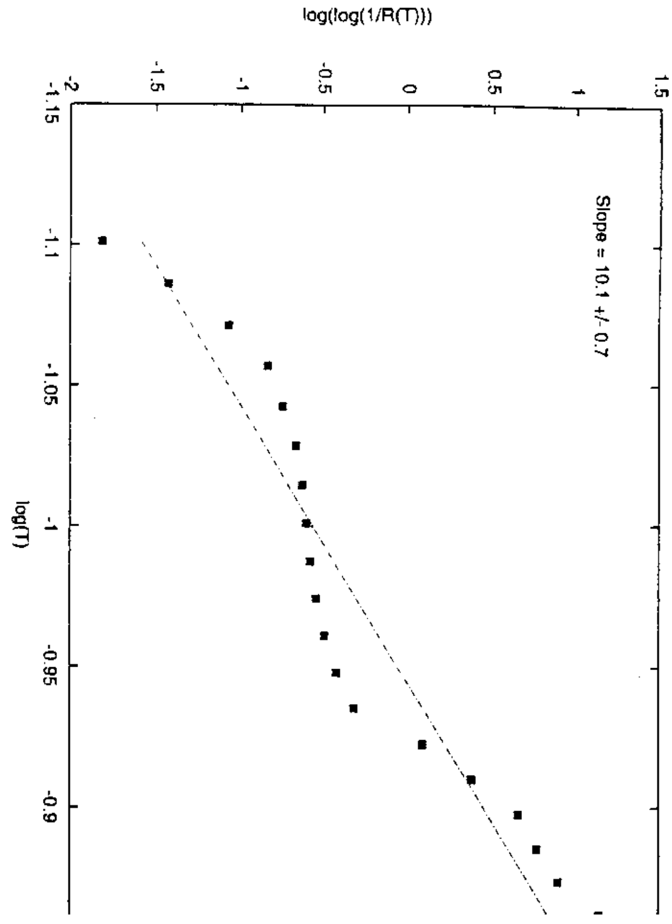

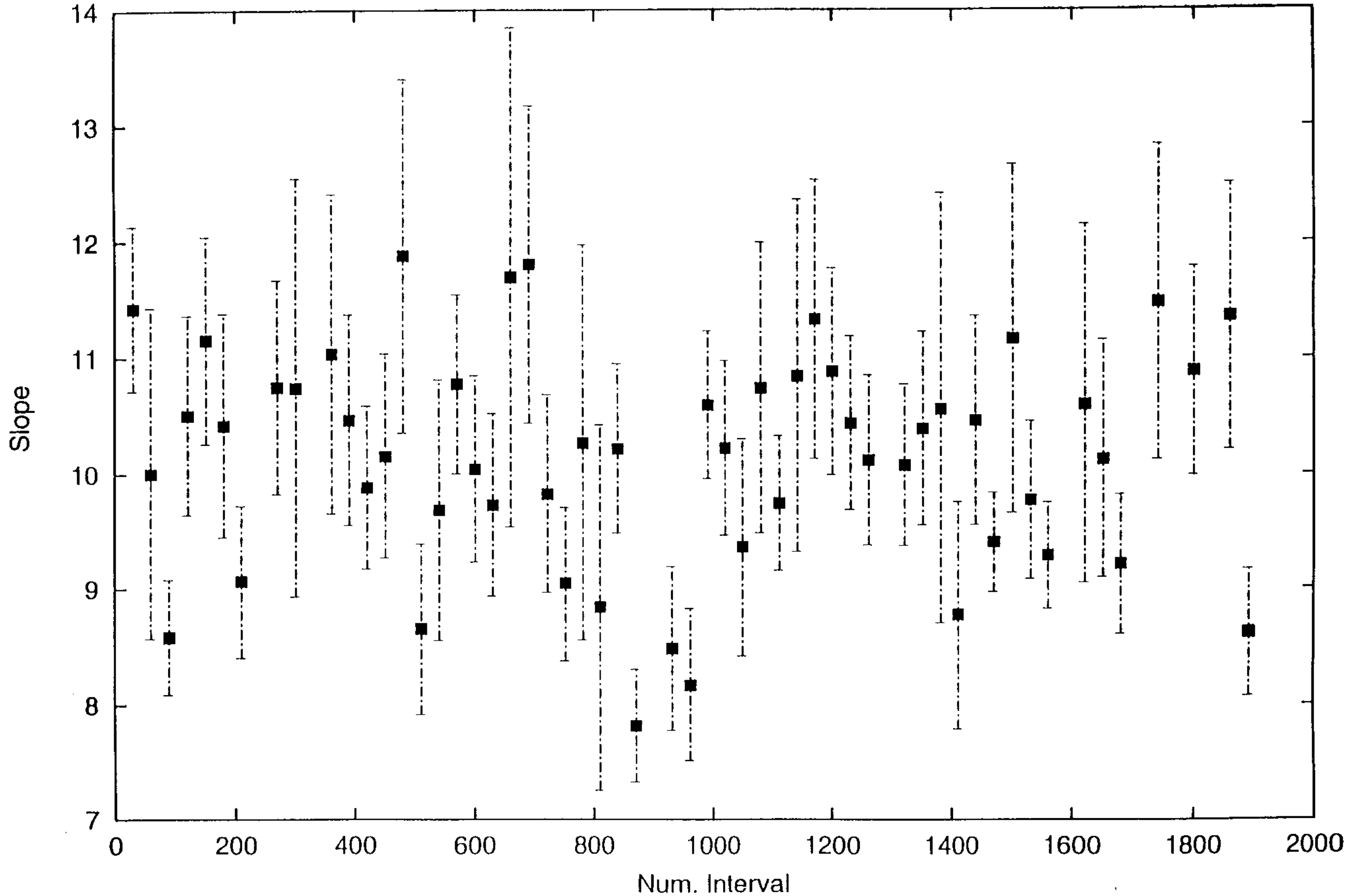

Slope
Num. Interval

Hallmarks of Self-Organized Criticality

Features	Sandpiles	Earthquakes
Boundary condition	constant "grain" rate	constant strain rate
Critical parameter	repose angle θ_c	tectonic stress σ_c
Dynamic fluctuation	small fluctuation in angle, $\Delta\theta_c \ll \theta_c$	small stress drop, $\Delta\sigma_c \ll \sigma_c$
Power law distribution	avalanche volume or energy	source length, seismic moment, energy (Gutenberg-Richter law)

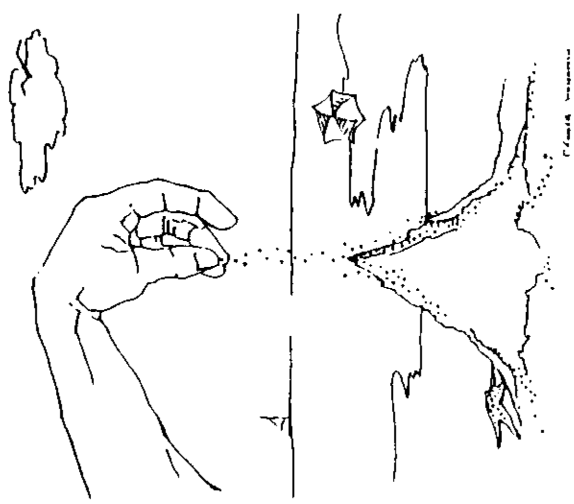

$$Z_i \longrightarrow Z_i - Z_c$$

$$Z_{nn} \longrightarrow +Y_i$$

EARTHQUAKE OCCURRENCE AS CRITICAL PHENOMENA

- the distribution of almost all properties of earthquakes are self-similar, *i.e.*, follow a power law

- action at distance

- these are the characteristics of critical phenomena that occur at phase transitions order/disorder

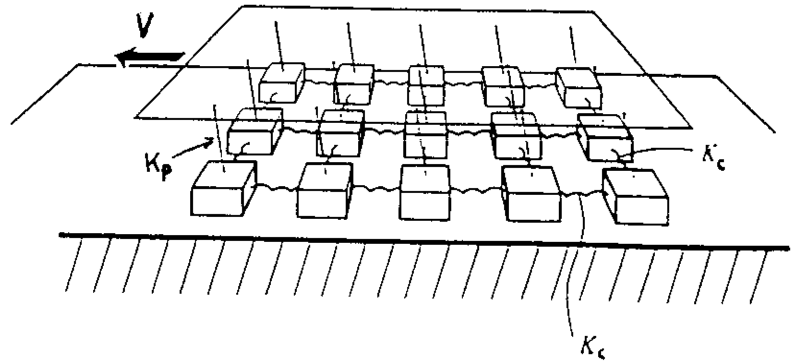

The Burridge–Knopoff spring–block model.

$$m\ddot{X} = K_c(X_{i+1} - 2X_i + X_{i-1}) - K_p(X_i - Vt) - F_p(\dot{X}_i)$$

$$F_{i,j} \longrightarrow F_{i,j} - F_c$$
$$F_{nn} \longrightarrow F_{nn} + \alpha F_c$$

$$F_{i,j} \longrightarrow 0$$
$$F_{nn} \longrightarrow F_{nn} + \alpha F_c$$

$$F_{i,j} \longrightarrow 0$$
$$F_{nn} \longrightarrow F_{nn} + \alpha F_{i,j}$$

PHENOMENOLOGY OF EARTHQUAKES AND FAULT POPULATION (Main, 1966)

1. Fault populations are broadly scale-invariant over several orders of magnitude (power law distribution).
2. Earthquake frequency-magnitude statistics also imply power law scaling (Gutenberg-Richter law).
3. Earthquakes have a relatively constant and relatively small stress drop over a wide range of scales during dynamic slip (3 MPa compared with tectonic stress, $\sim 10 - 100$ MPa .
4. Fault and fracture breaks are rough, with self-affine or self-similar scaling.
5. Earthquake population in diverse tectonic zones exhibit spatial variability, clustering and intermitency, quantitatively consistent with multifractal scaling.
6. The distribution of spacings of hypocentral locations of earthquakes and laboratori acoustic emissions are power law in both space and time.
7. Earthquakes have aftershock sequences that decay at a rate $R(t)$ determined by Omori's law $R(t) = \frac{R_0}{(t+t_0)^p}$, where p is a power law index and R_0 and t_0 are constants.
8. Seiswmicity can be induced by stress pereturbations smaller than the stress drop in individual events; i.e., earthquakes can be "triggered".

SEISMIC CATALOG

Is characterized by <u>three temporal scales</u>.

Assume, for example, an earthquake of magnitude

$$M_w \sim 7$$

- period of recurrence: 100 years	$\sim 10^9 s$
- aftershock duration: 1 year	$\sim 10^7 s$
- rupture time: 1 - 2 minutes	$\sim 10^2 s$

Renormalysing

$\sim 10^7 s$

$\sim 10^5 s$

$\sim 10^0 s$

EARTHQUAKE OCCURRENCE AS CRITICAL PHENOMENA

- **the distribution of almost all properties of earthquakes are <u>self-similar</u>, *i.e.*, follow a power law**
- **action at distance**

- **these are the characteristics of critical phenomena that occur at phase transitions order/disorder**

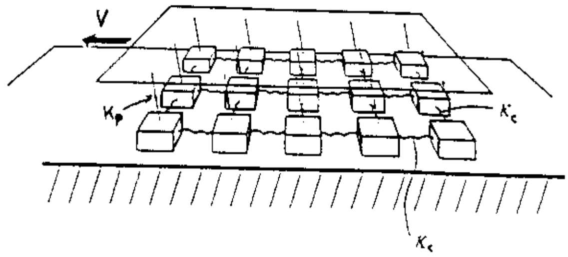

The Burridge-Knopoff spring-block model.

$$m\ddot{X} = K_c(X_{i+1} - 2X_i + X_{i-1}) - K_p(X_i - Vt) - F_p(X_i)$$

$$F_{i,j} \longrightarrow F_{i,j} - F_c$$
$$F_{nn} \longrightarrow F_{nn} + \alpha F_c$$

$$F_{i,j} \longrightarrow 0$$
$$F_{nn} \longrightarrow F_{nn} + \alpha F_c$$

$$F_{i,j} \longrightarrow 0$$
$$F_{nn} \longrightarrow F_{nn} + \alpha F_{i,j}$$

P. Bak / Self-organized criticality

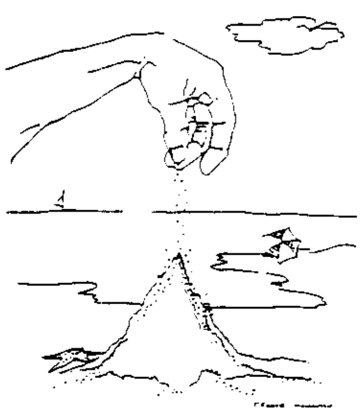

$$Z_i \longrightarrow Z_i - Z_c$$
$$Z_{nn} \longrightarrow +Y_i$$

Hallmarks of Self-Organized Criticality

Features	Sandpiles	Earthquakes
Boundary condition	constant "grain" rate	constant strain rate
Critical parameter	repose angle θ_c	tectonic stress σ_c
Dynamic fluctuation	small fluctuation in angle, $\Delta\theta_c \ll \theta_c$	small stress drop, $\Delta\sigma_c \ll \sigma_c$
Power law distribution	avalanche volume or energy	source length, seismic mome energy (Gutenberg-Richter

MINIMALIST MODEL

Is a *toy* model designed to describe an extended system with active propagating particles interacting with other active or passive static particles. Starting from a homogeneous *mass* distribution of *active* and *passive* cells, the system evolves to a *self-organized critical state*.

Define a regular 2-D lattice. The cells of this larttice might be found in three possible states: *active*, *passive* or *empty*.

In short, the equivalence can be stated as follows:

passive cell $\longleftrightarrow$ broken asperity

active cell $\longleftrightarrow$ asperity ready to break

annihilated cell $\longleftrightarrow$ healed slip

The equivalence between the minimalist model and the flow of seismicity can be clearly stated in terms of a model of nucleation and origin of seismicity developed by Cochard and Madariaga (1994, 1996).

These authors modeled the dynamics of the faulting through a rate-dependent friction law, and starting from an homogeneous initial stress distribution, found that when friction is strongly rate dependent, the healing process destabilizes producing premature healing of slip and partial stress drop, that in turn results in large variations of the state of the stress.

As noted by Cochard and Madariaga (1996), the rupture propagation "adjusts" itself to satisfy a scaling law, suggesting that a state resembling that of self-organized criticality has been reached.

ULES FOR UPDATING THE SYSTEM FROM IME t TO TIME $t+1$

.) Active cells at t *burn out* and become passive at time $t+1$.

!) Passive cells are annihilated when they have one, and only one, active neighbor.

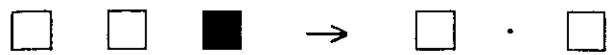

i) Active cells are created from empty cells when they have one, and only one, active neighbor, which must have a passive cell at the opposite direction.

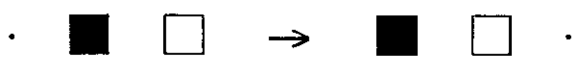

ROPAGATION

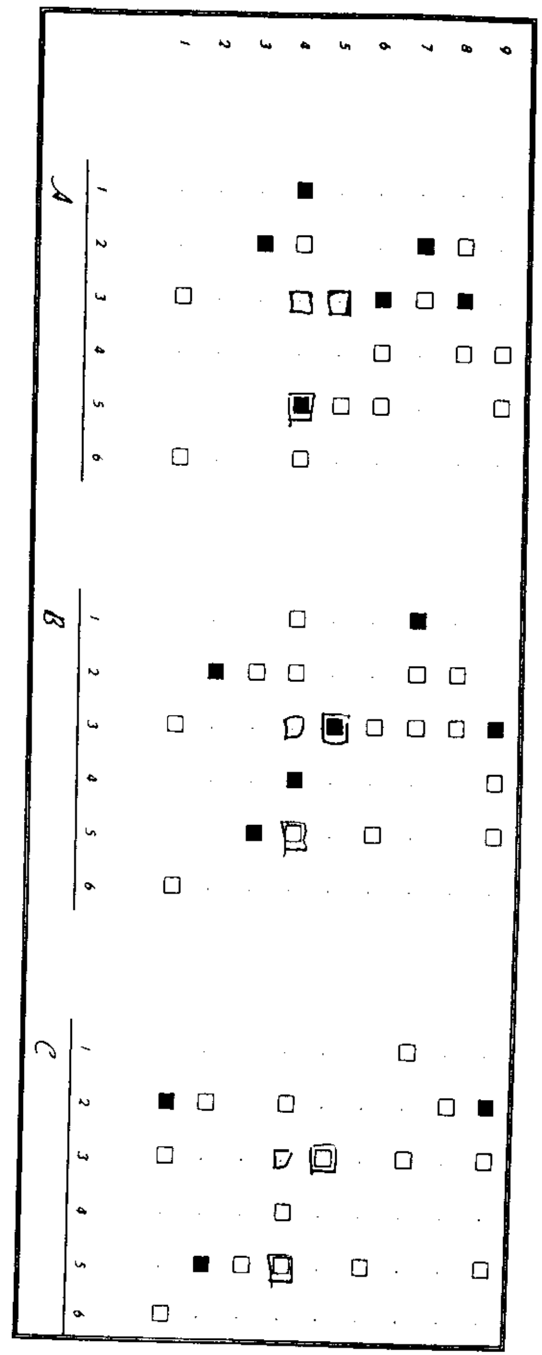

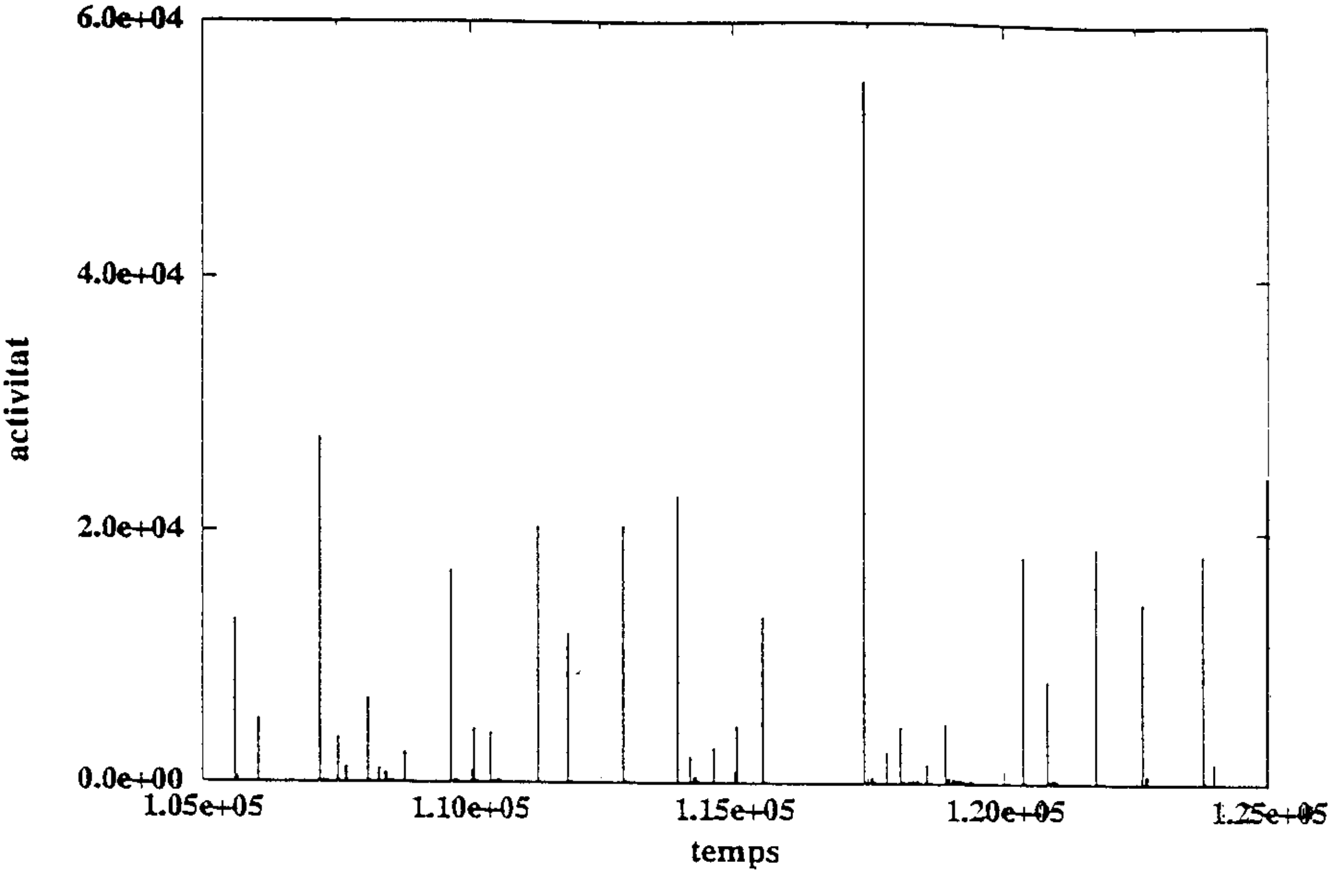
6.0e+04
4.0e+04
2.0e+04
0.0e+00
activitat
1.05e+05
1.10e+05
1.15e+05
1.20e+05
1.25e+05
temps

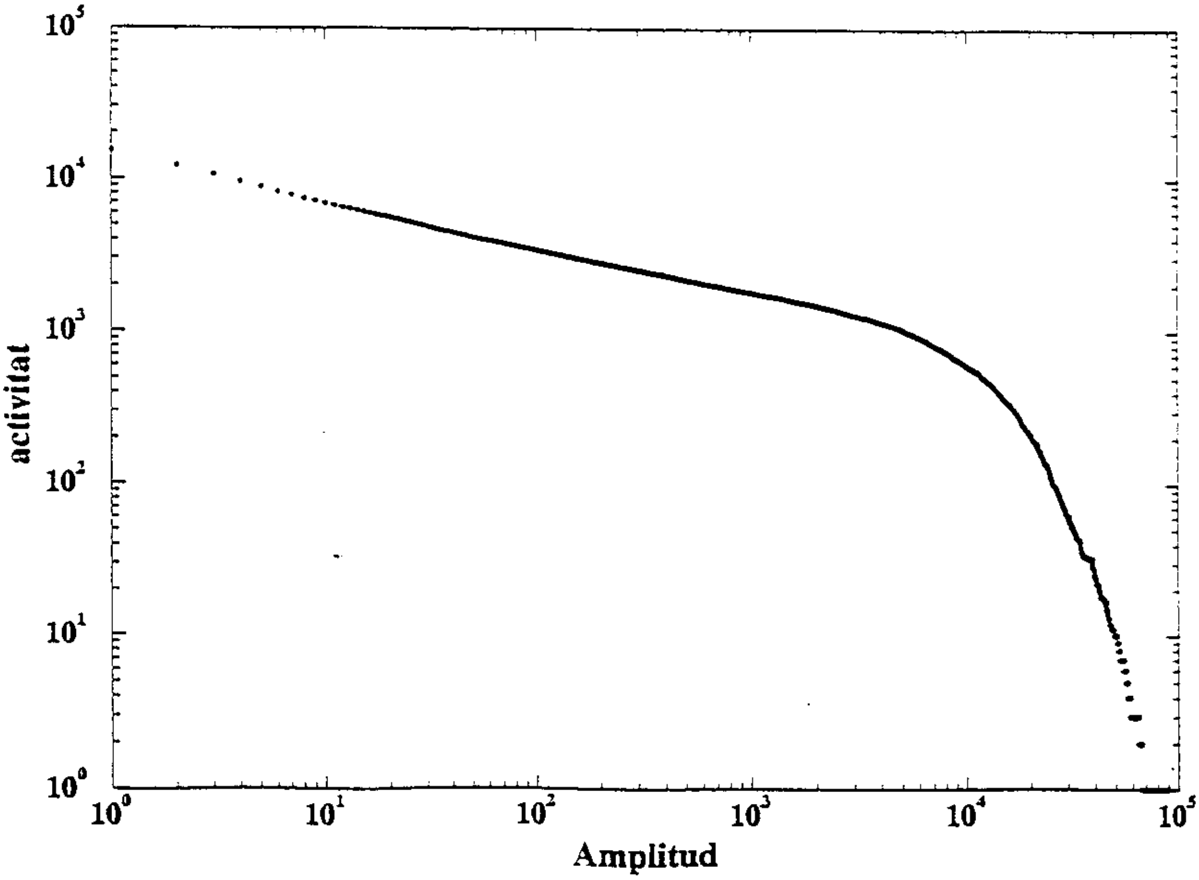
10^5
10^4
10^3
10^2
10^1
10^0
activitat
10^0
10^1
10^2
10^3
10^4
10^5
Amplitud

Per Bak (1990). Self-organized criticality
Physica A, 163, 403-409

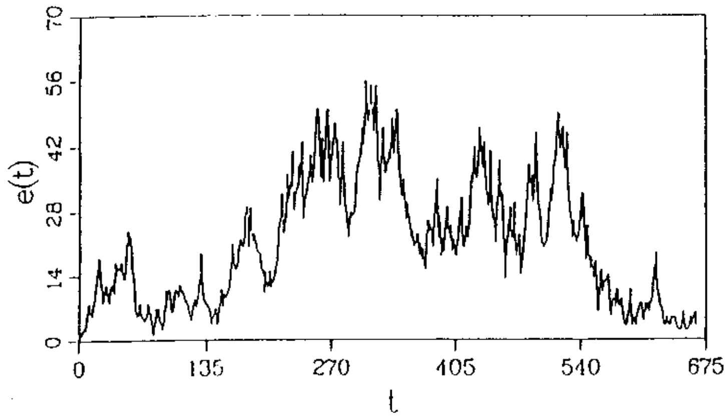

Fig. 3. Temporal evolution of activity (energy release) during a single avalanche or earthquake.

50 x 50

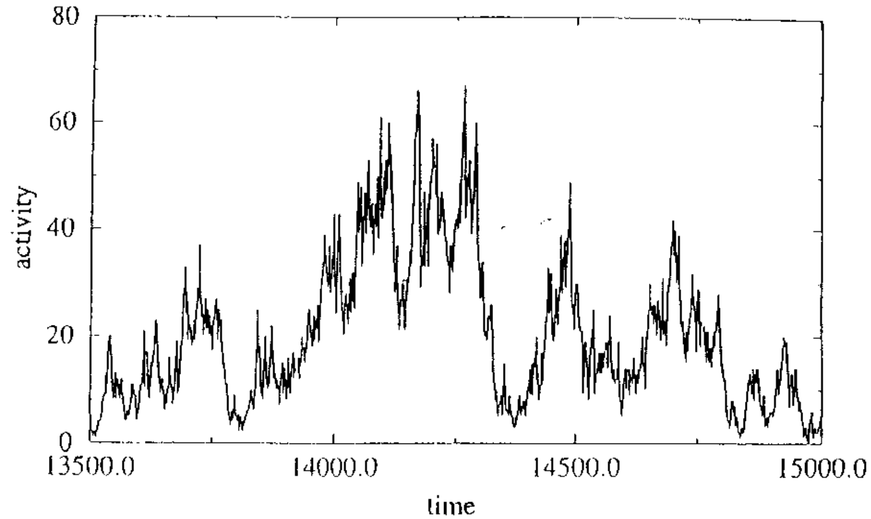

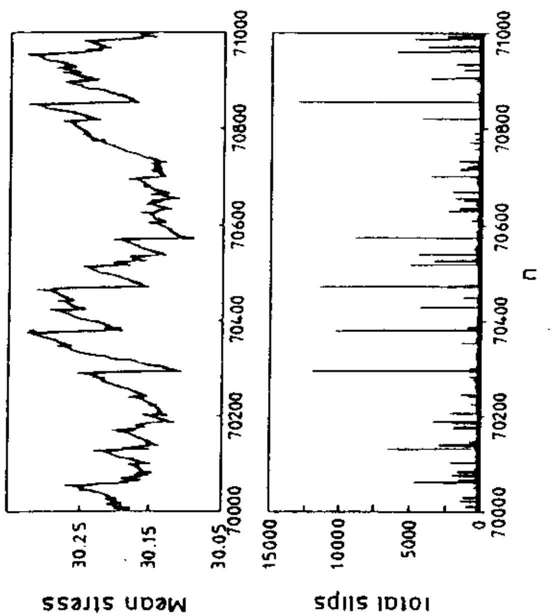

Gross, Klein & Rundle (1996) — B-K model

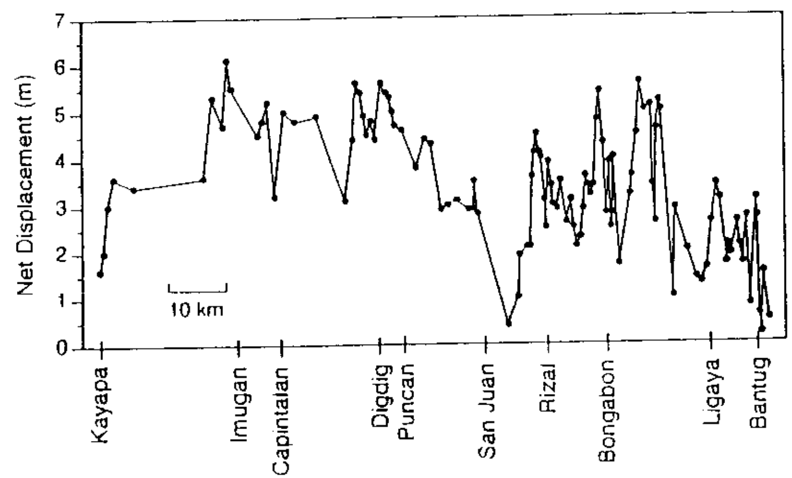

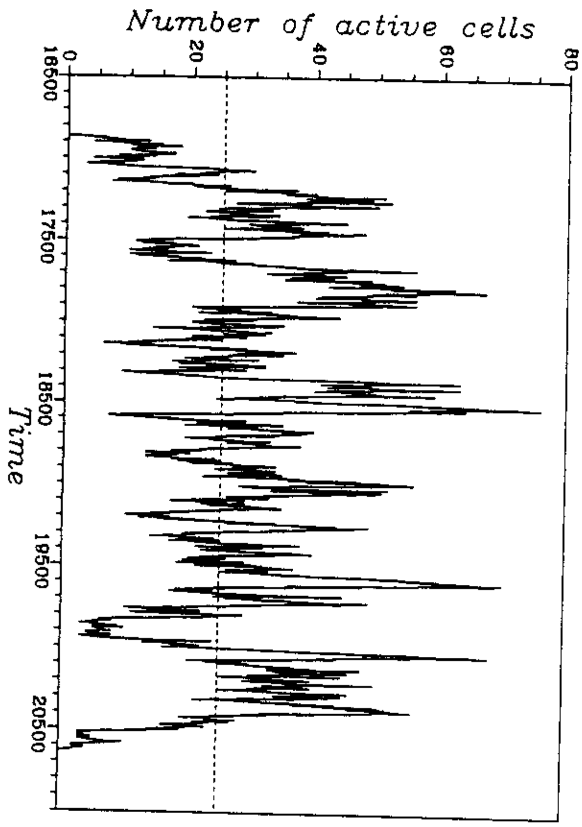

CELLULAR AUTOMATA

1. Configure intial conditions of the grid

2. Add a unit energy to a random site of the grid.
   - look for the energy of the site exceeds or not a given threshold:
   - If YES, call RELAX. GOTO 2.
   - ELSE, GOTO 2

SUBROUTINE RELAX

- explore the entire grid and update where needed
- stgrength of the event (cascade): total number of units of energy

TIME SCALES - cascades: $\ll$ inter-event time
- cascades: instantaneous

- each cascade is an independent event (a step in the loop)
- no aftershocks
- small cascades cannot be assimilated to noise

SEISMIC CATALOG

- remove clustering (foreshocks and aftershocks)
- are the remaining earthquakes independent events?
- which of them, if any, can be considered as noise?
- the results of the statistics applied to cellular automata and seismiccatalogs, are comparable?

Predicting natural hazards resembles the game of croquet in *Alice in Wonderland*, where the ball was a live hedgehog who would not stand still or go where the players intended. We can make statistics about the habits of hedgehogs, but we are still far from understanding the rules of the game.

(Cinna Lomnitz)

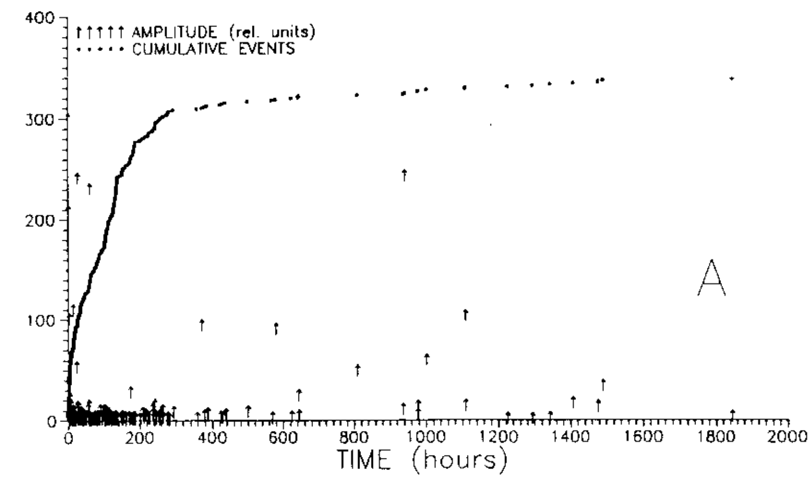

↑↑↑↑↑ AMPLITUDE (rel. units)
• • • • • CUMULATIVE EVENTS
A
TIME (hours)

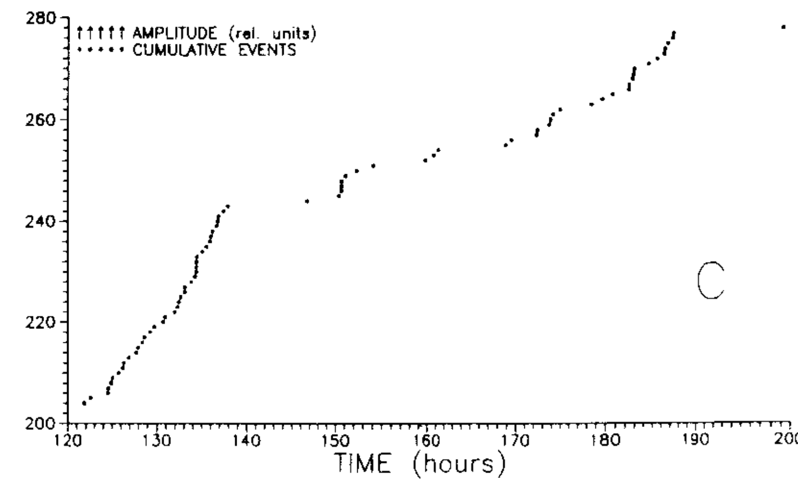

↑↑↑↑↑ AMPLITUDE (rel. units)
• • • • • CUMULATIVE EVENTS
C
TIME (hours)

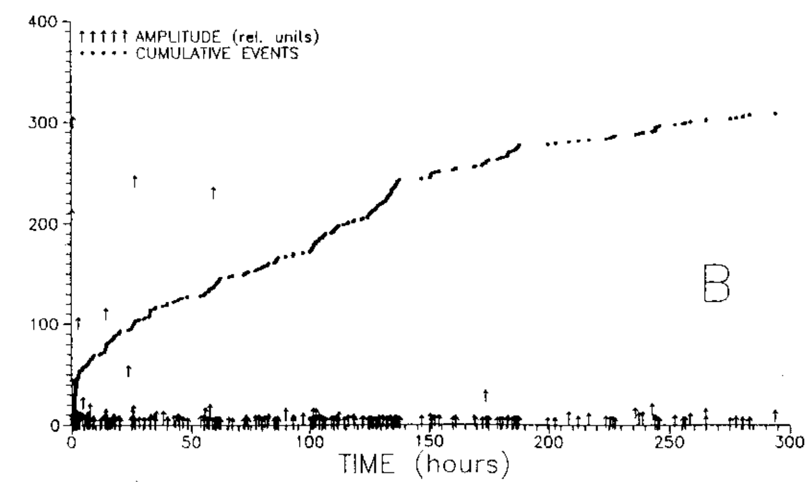

↑↑↑↑↑ AMPLITUDE (rel. units)
• • • • • CUMULATIVE EVENTS
B
TIME (hours)

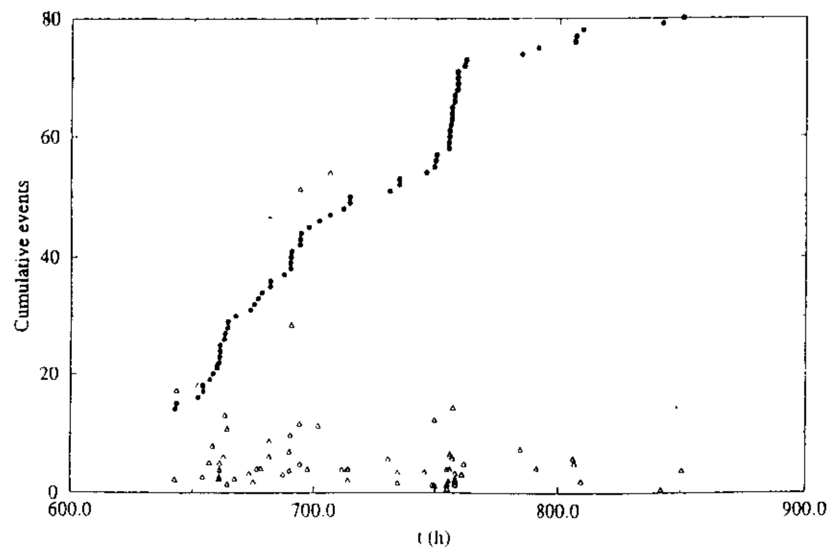

Cumulative events
t (h)

Modified Omori's law

$$R = \frac{K}{(t+c)^p}, \tag{1}$$

R: occurrence rate of aftershocks

t: time

K, c, p: constants

The cumulative number of aftershocks $N(t)$, defined as $N(t) = \int_0^t n(s)ds$ is

$$N(t) = \frac{K\left[c^{(1-p)} - (c+t)^{(1-p)}\right]}{(p-1)} \tag{2}$$

Mean Earthquake Recurrence Time:

can forecast the average time between large events.

Seismicity Rate

$$R = \frac{r\dot{\tau}/\dot{\tau}_r}{\left[\frac{\dot{\tau}}{\dot{\tau}_r}\exp\left(-\frac{\Delta\tau}{A\sigma}\right) - 1\right]\exp\left[-\frac{t}{t_a}\right] + 1} \tag{3}$$

R: seismicity rate

r: the reference seismicity rate,

$\dot{\tau}_r$ and $\dot{\tau}$: stressing rate prior and following the stress step

$\Delta\tau$: earthquake stress change

A a fault constitutive parameter

σ the normal stress

t time

t_a *aftershock duration.*

Eq. (3) gives Omori's law for $t/t_a < 1$.

The mean earthquake recurrence time t_r can be approximated as

$$t_r = t_a \frac{-\Delta\tau}{A\sigma}. \tag{4}$$

If we define

$$T = \frac{\dot{\tau}}{\dot{\tau}_r}, \quad B = \left[\frac{\dot{\tau}}{\dot{\tau}_r}\exp\left(-\frac{\Delta\tau}{A\sigma}\right) - 1\right], \quad C = t_a.$$

then eq.(3) can be integrated to obtain the cumulative function

$$F(t) = TC\ln\left[\frac{\exp(t/C) + B}{1+B}\right], -1 \le B \le 0. \tag{5}$$

which can be fitted to data to obtain t_a and t_r.

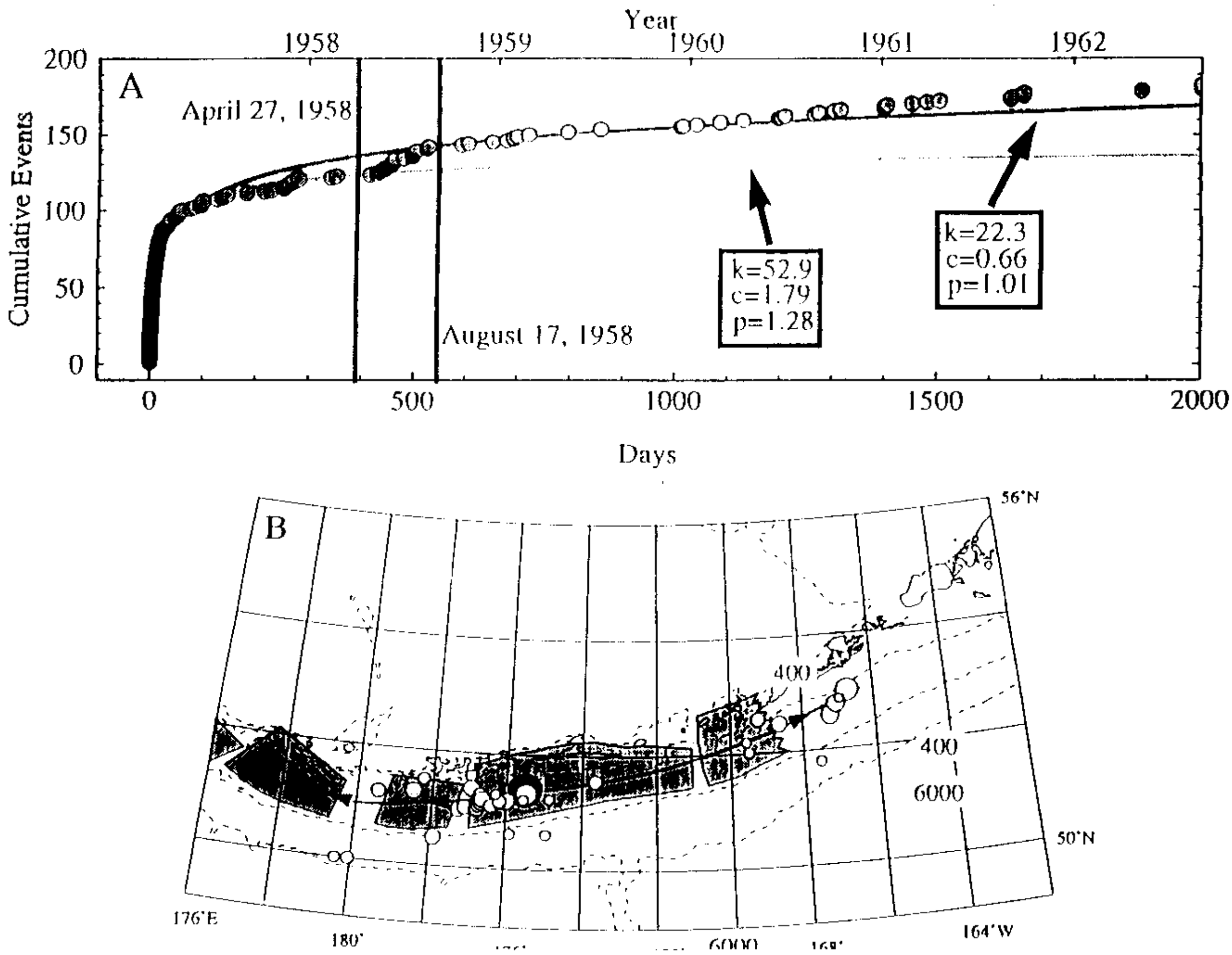
Year
1958
1959
1960
1961
1962
A
April 27, 1958
August 17, 1958
k=52.9
c=1.79
p=1.28
k=22.3
c=0.66
p=1.01
Cumulative Events
Days
B
56°N
50°N
176°E
180°
164°W
400
6000

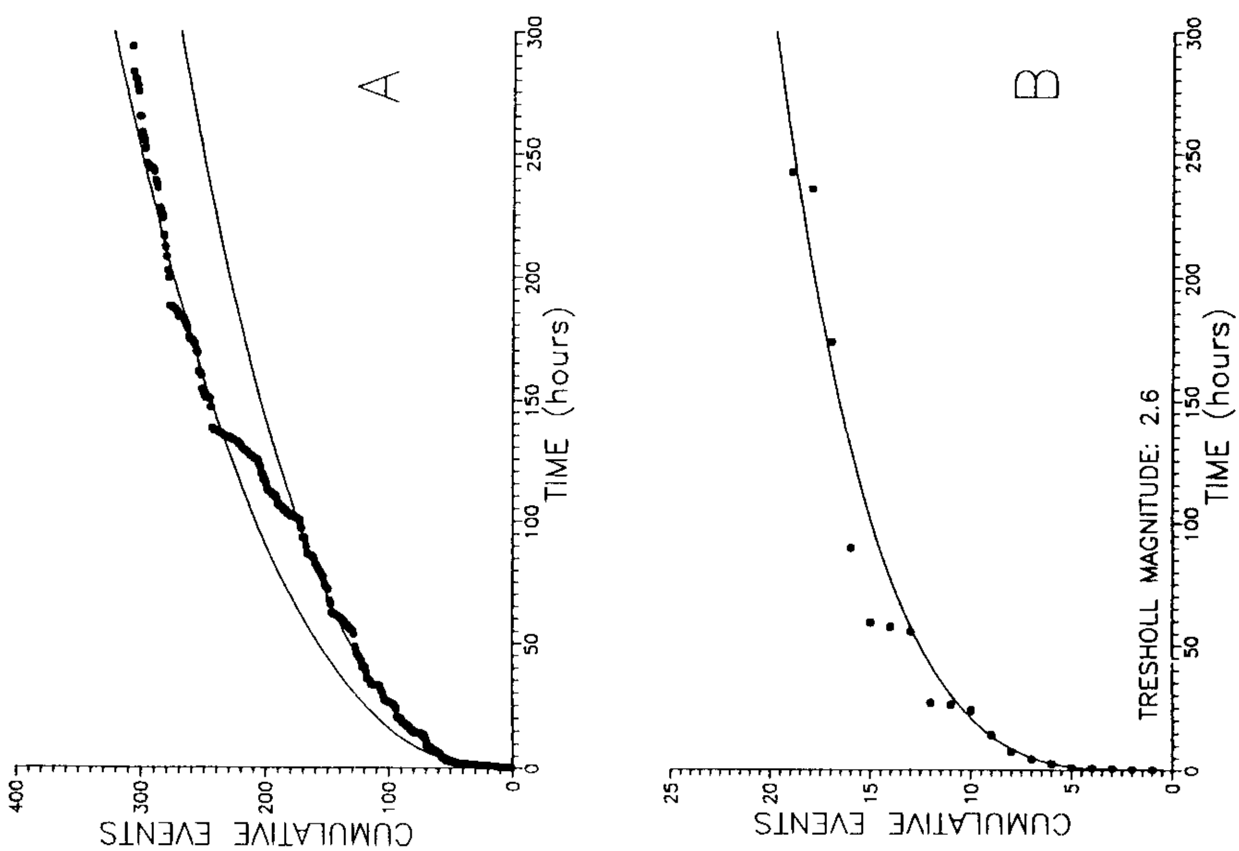
A
B
CUMULATIVE EVENTS
TIME (hours)
TRESHOLL MAGNITUDE: 2.6

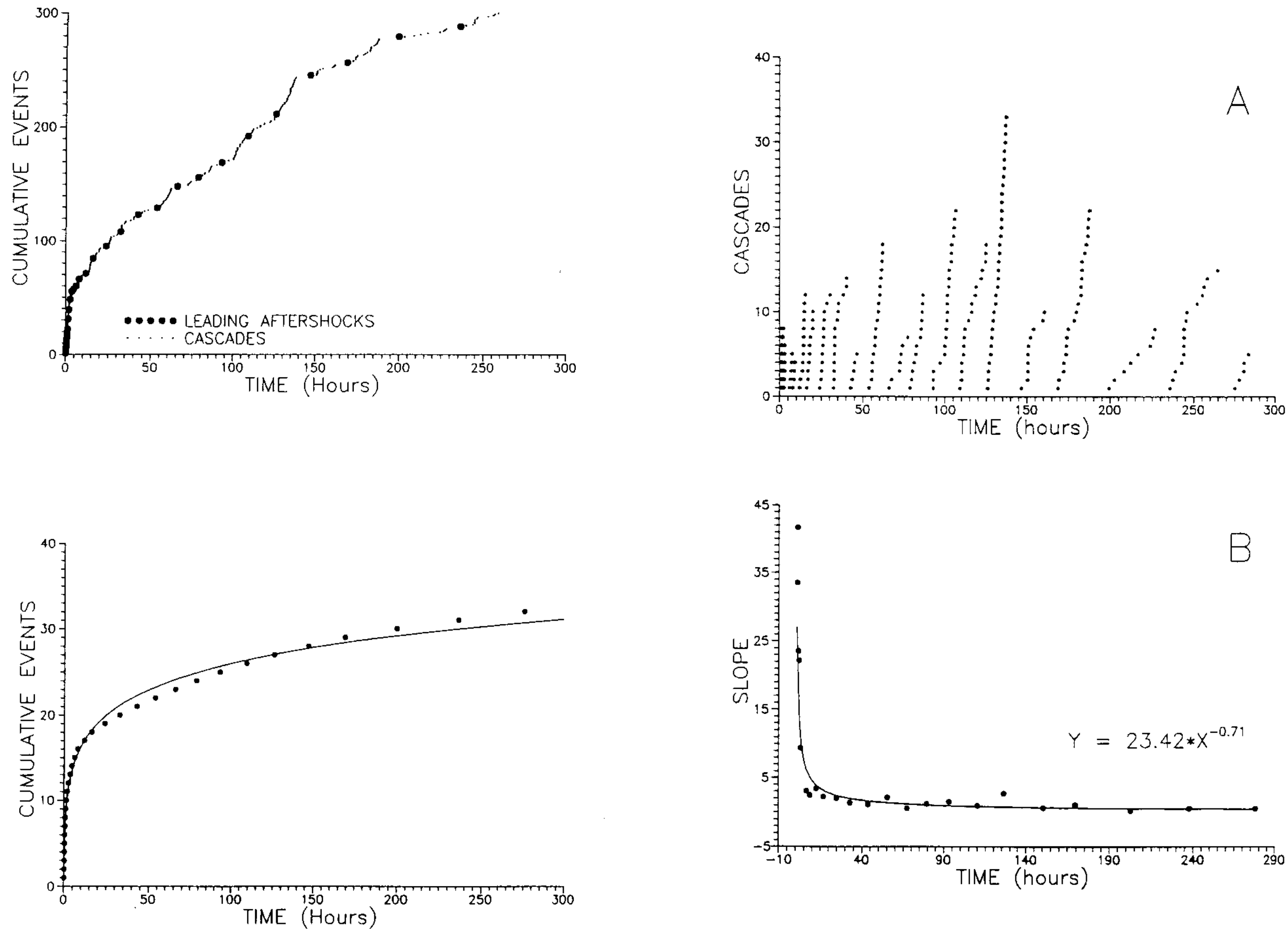

CUMULATIVE EVENTS
LEADING AFTERSHOCKS
CASCADES
TIME (Hours)
CASCADES
TIME (hours)
A
CUMULATIVE EVENTS
TIME (Hours)
SLOPE
Y = 23.42*X^-0.71
TIME (hours)
B

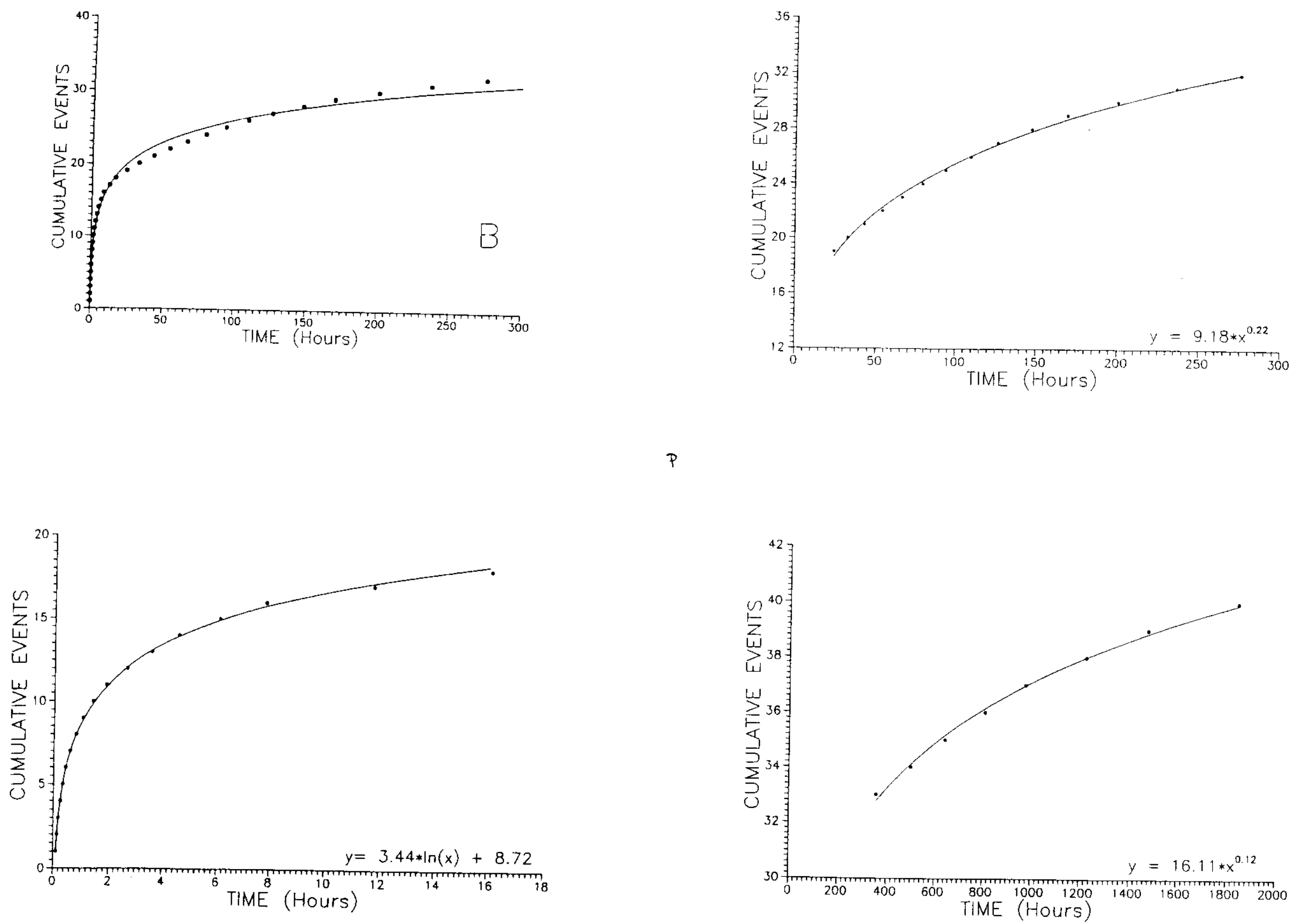

CUMULATIVE EVENTS
TIME (Hours)
B
y = 9.18*x^0.22
y= 3.44*ln(x) + 8.72
y = 16.11*x^0.12

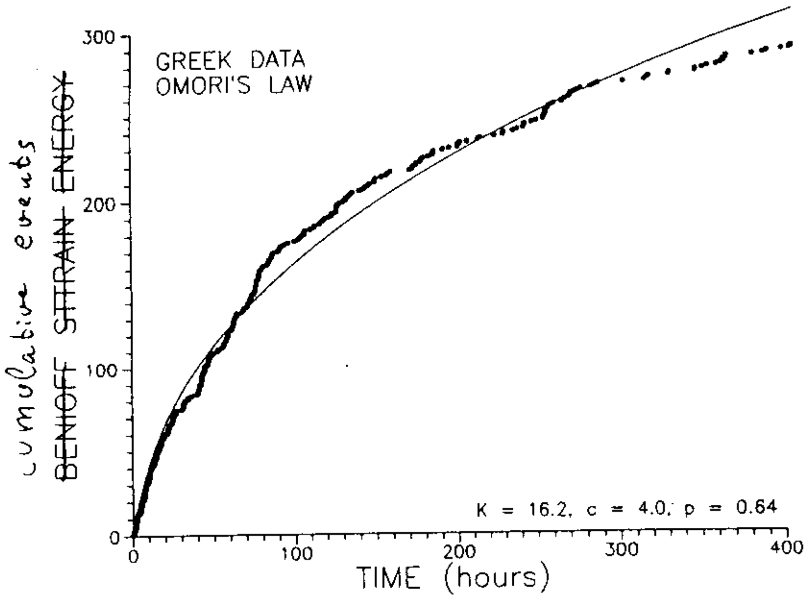
GREEK DATA
OMORI'S LAW
cumulative events
BENIOFF STTRAIN ENERGY
K = 16.2, c = 4.0, p = 0.64
TIME (hours)

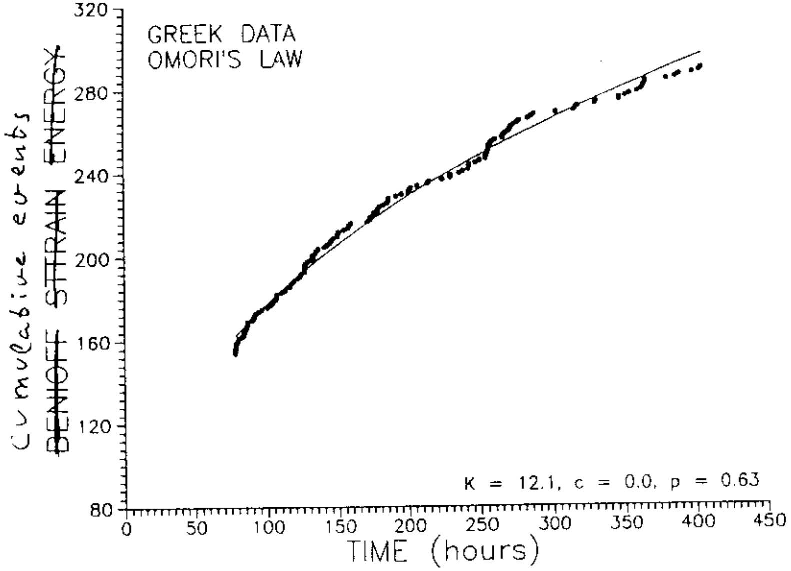
GREEK DATA
OMORI'S LAW
cumulative events
BENIOFF STTRAIN ENERGY
K = 12.1, c = 0.0, p = 0.63
TIME (hours)

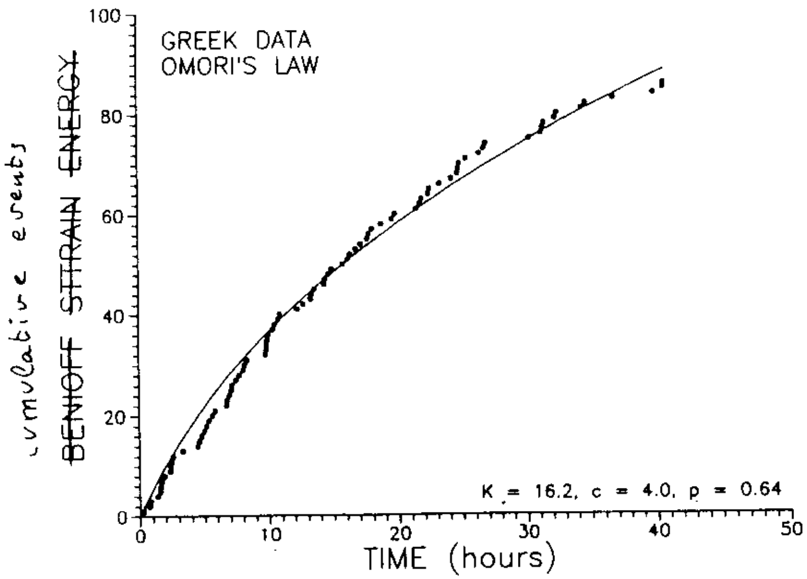
GREEK DATA
OMORI'S LAW
cumulative events
BENIOFF STTRAIN ENERGY
K = 16.2, c = 4.0, p = 0.64
TIME (hours)

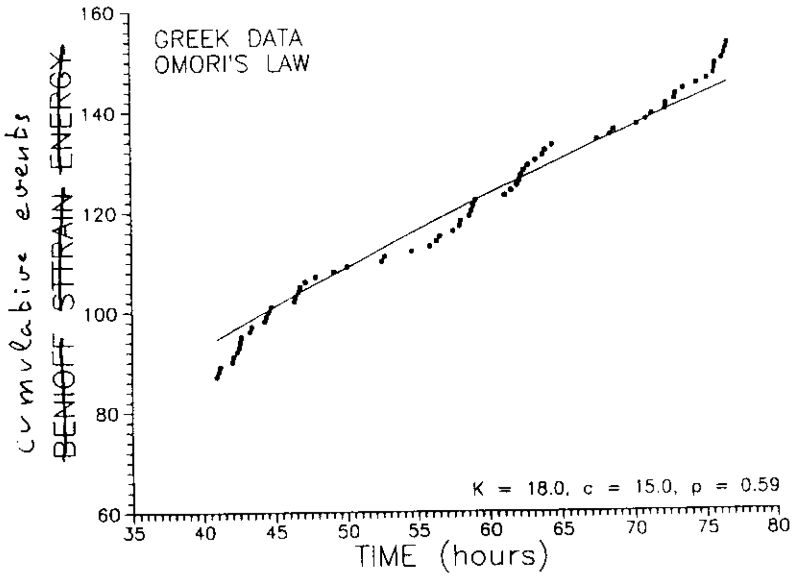
GREEK DATA
OMORI'S LAW
cumulative events
BENIOFF STTRAIN ENERGY
K = 18.0, c = 15.0, p = 0.59
TIME (hours)

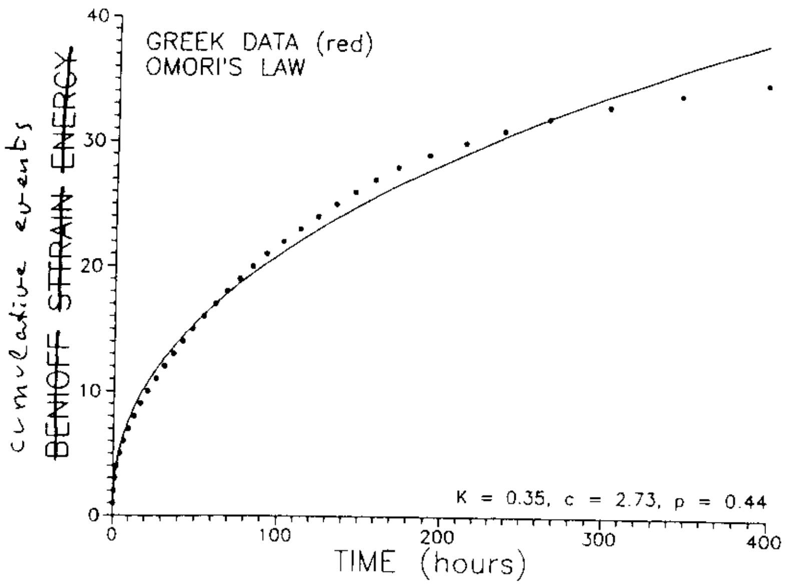
cumulative events
~~BENIOFF STTRAIN ENERGY~~
GREEK DATA (red)
OMORI'S LAW
K = 0.35, c = 2.73, p = 0.44
TIME (hours)

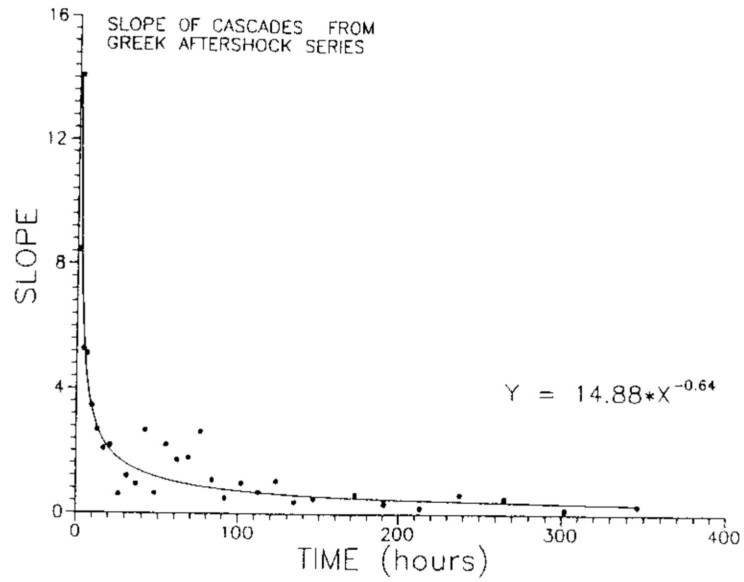
SLOPE OF CASCADES FROM
GREEK AFTERSHOCK SERIES
SLOPE
$Y = 14.88*X^{-0.64}$
TIME (hours)

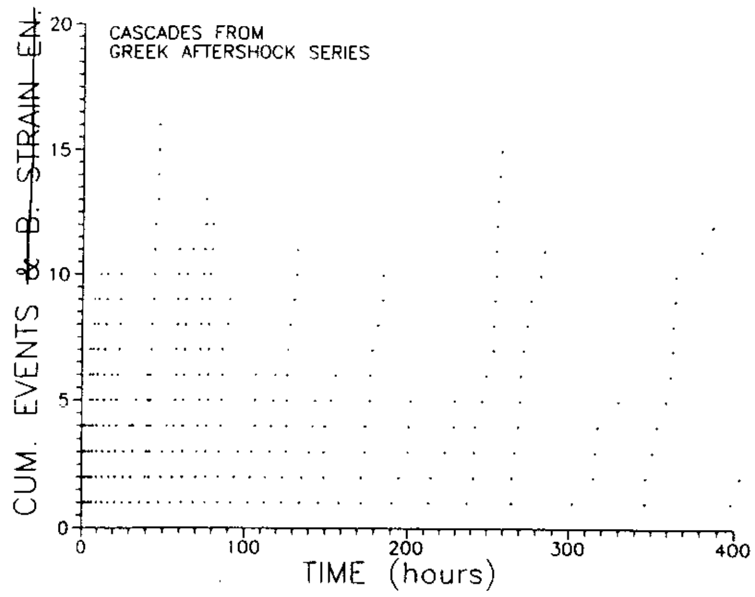
CUM. EVENTS ~~& B. STRAIN EN.~~
CASCADES FROM
GREEK AFTERSHOCK SERIES
TIME (hours)

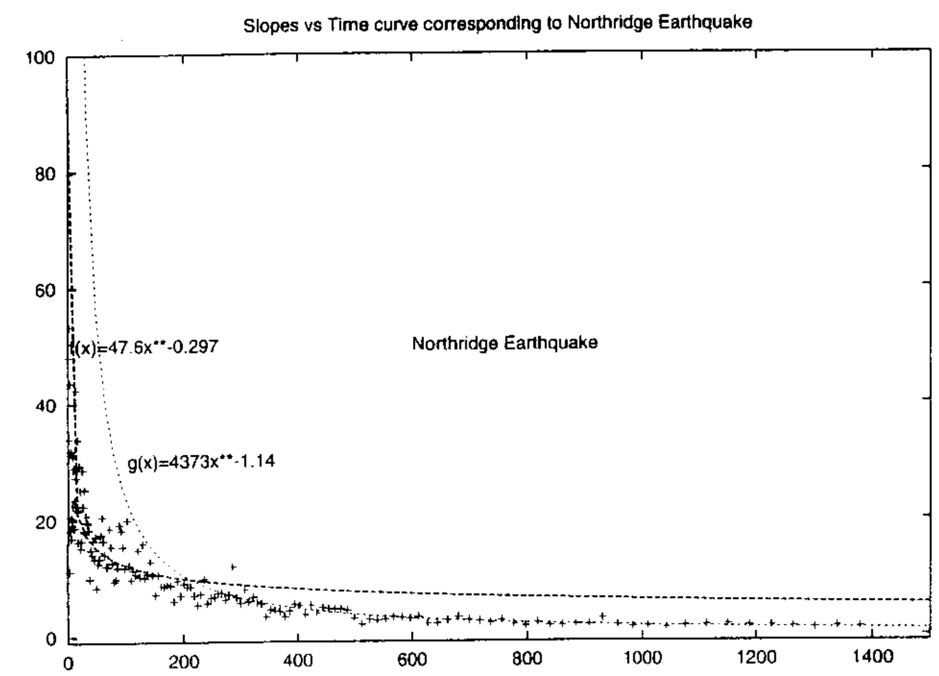
Slopes vs Time curve corresponding to Northridge Earthquake
Northridge Earthquake
f(x)=47.6x**-0.297
g(x)=4373x**-1.14

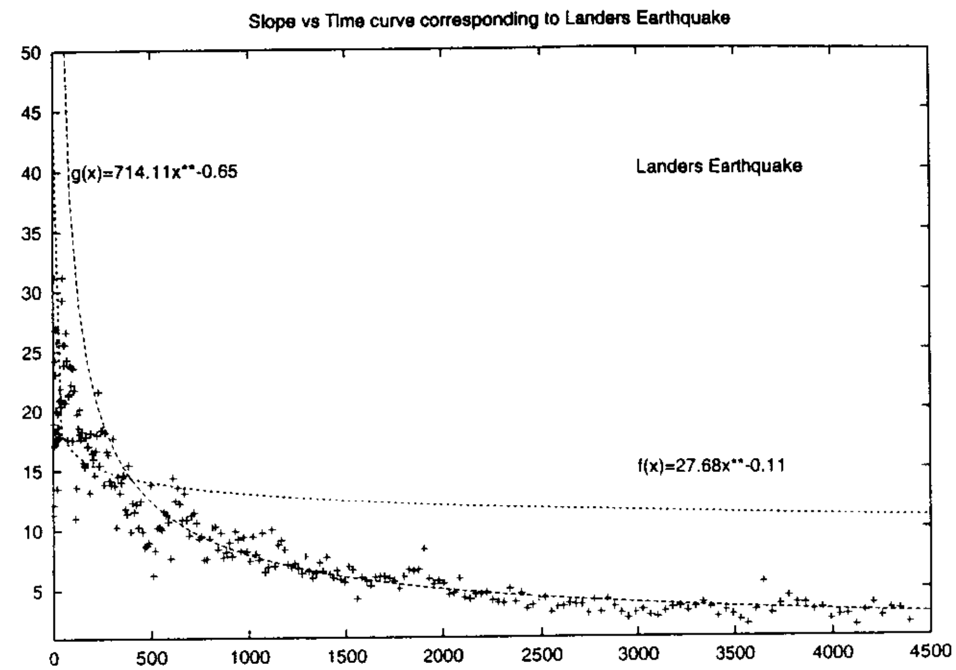
Slope vs Time curve corresponding to Landers Earthquake
Landers Earthquake
g(x)=714.11x**-0.65
f(x)=27.68x**-0.11

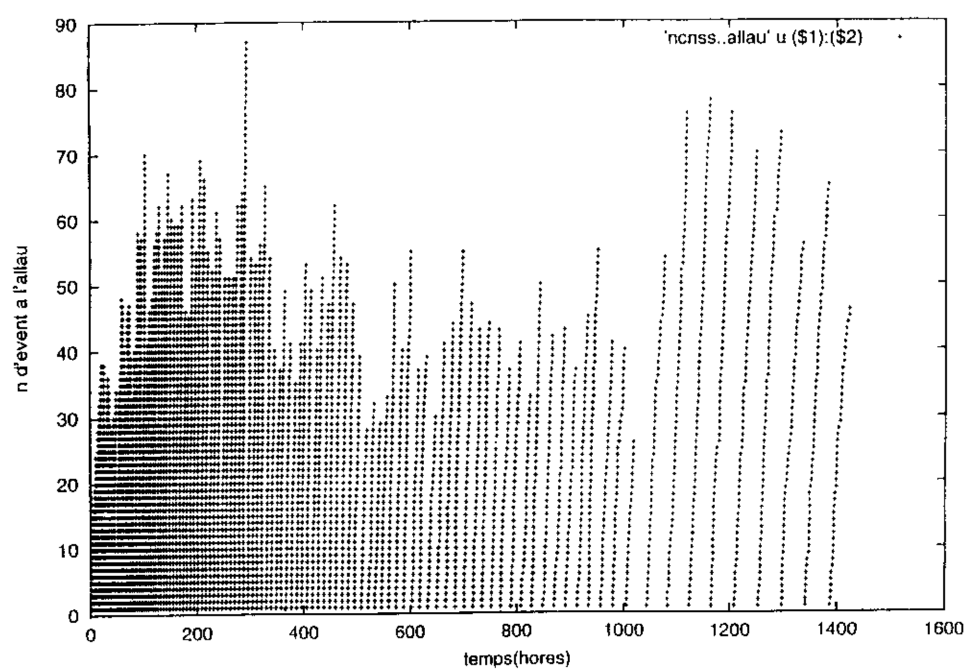
'ncnss..allau' u ($1):($2)
n d'event a l'allau
temps(hores)

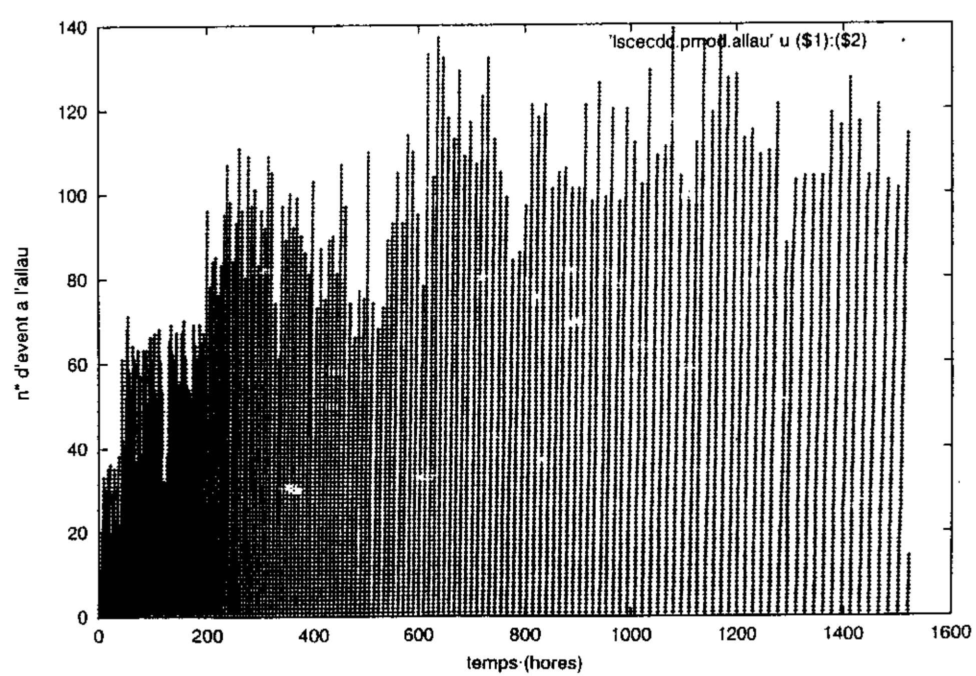
'lscecdd.pmod.allau' u ($1):($2)
n° d'event a l'allau
temps·(hores)

The power-law increase in regional seismicity before large events was first documented by BUFE and VARNES (1993) and BUFE *et al.* (1994) who found that the clustering of intermediate events before a large shock produces an increase in cumulative regional energy release (or in cumulative regional Benioff strain, $\varepsilon(t) = \Sigma_{j=1}^{N(t)} E_j^{1/2}$) that can be fit by a power law time-to-failure relation of the form

$$\varepsilon(t) = A + B(t_c - t)^m \tag{1}$$

where t_c is the time of the large event, B is negative and m is usually about 0.3.

Another testable hypothesis that has emerged from the critical point model for seismicity is the possibility of log-periodic fluctuations in seismicity approaching criticality. SORNETTE and SAMMIS (1995) showed that if the spatial renormalization can only be made at a discrete fractal hierarchy of scale lengths, then the critical exponent is imaginary in time and Equation (1) becomes (to a first approximation, retaining only leading term in the periodicity)

$$\varepsilon(t) = A + B(t_c - t)^m\left[1 + C\cos\left(2\pi\frac{\log(t_c - t)}{\log\lambda} + \psi\right)\right]. \tag{3}$$

Such log-periodicity has been documented in several cases (SORNETTE and SAMMIS, 1995; VARNES and BUFE, 1996), but it has yet to be established as a universal precursor to large events. The modeling study presented below suggests that it may not be universal. However, if observed, log-periodicity allows a more precise estimate of t_c (SORNETTE and SAMMIS, 1995; SAMMIS *et al.*, 1996).

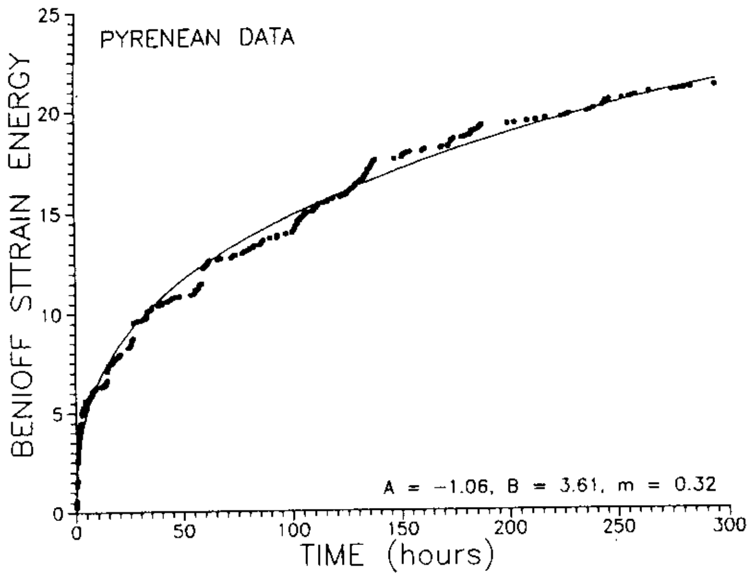
PYRENEAN DATA
BENIOFF STTRAIN ENERGY
TIME (hours)
A = -1.06, B = 3.61, m = 0.32

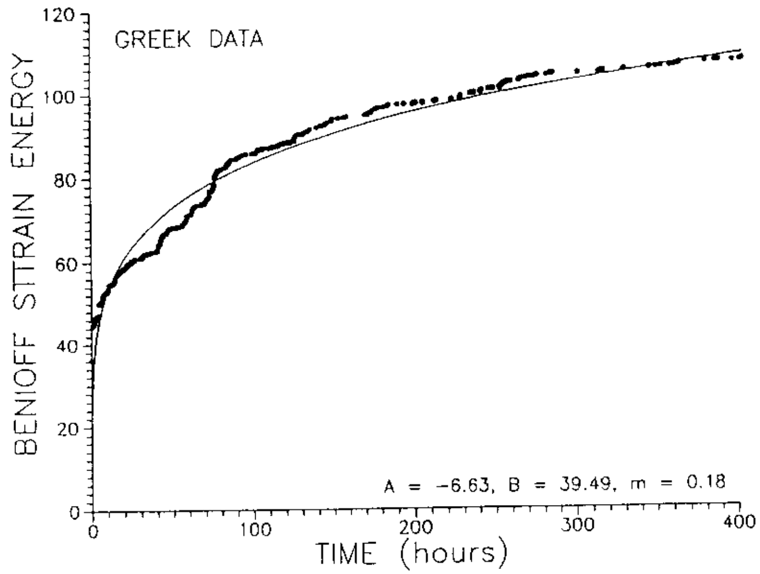
GREEK DATA
BENIOFF STTRAIN ENERGY
TIME (hours)
A = -6.63, B = 39.49, m = 0.18

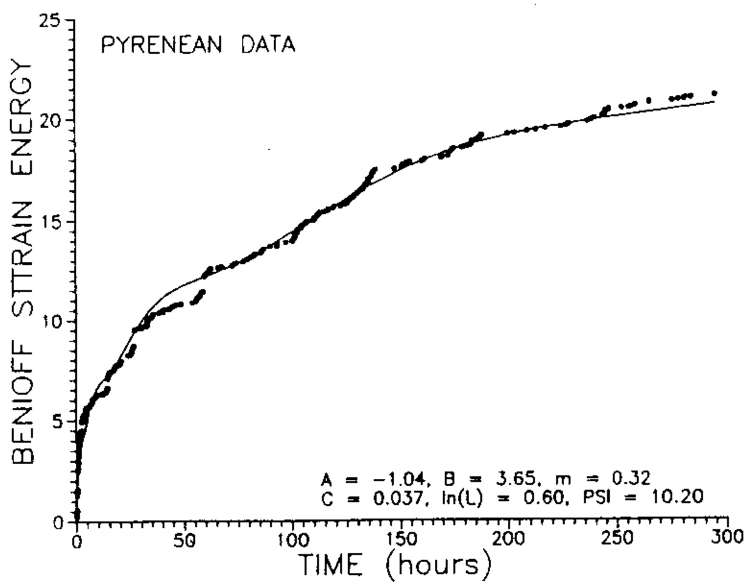
PYRENEAN DATA
BENIOFF STTRAIN ENERGY
TIME (hours)
A = -1.04, B = 3.65, m = 0.32
C = 0.037, ln(L) = 0.60, PSI = 10.20

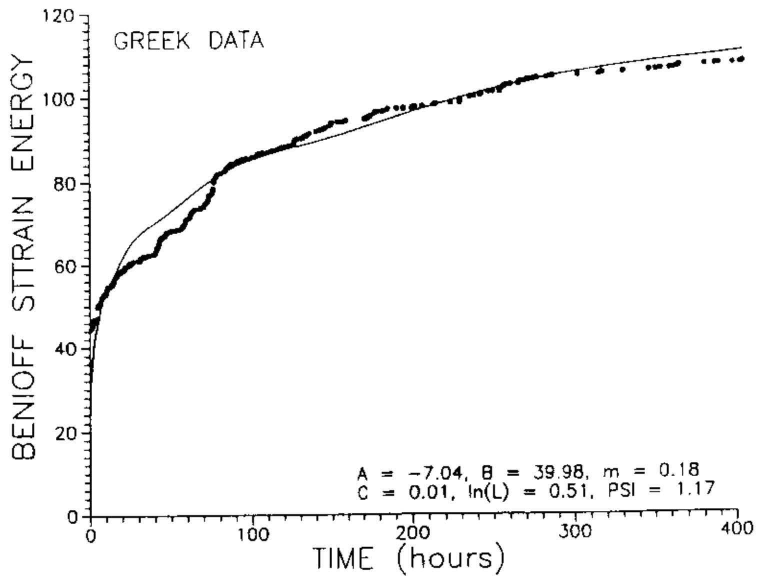
GREEK DATA
BENIOFF STTRAIN ENERGY
TIME (hours)
A = -7.04, B = 39.98, m = 0.18
C = 0.01, ln(L) = 0.51, PSI = 1.17

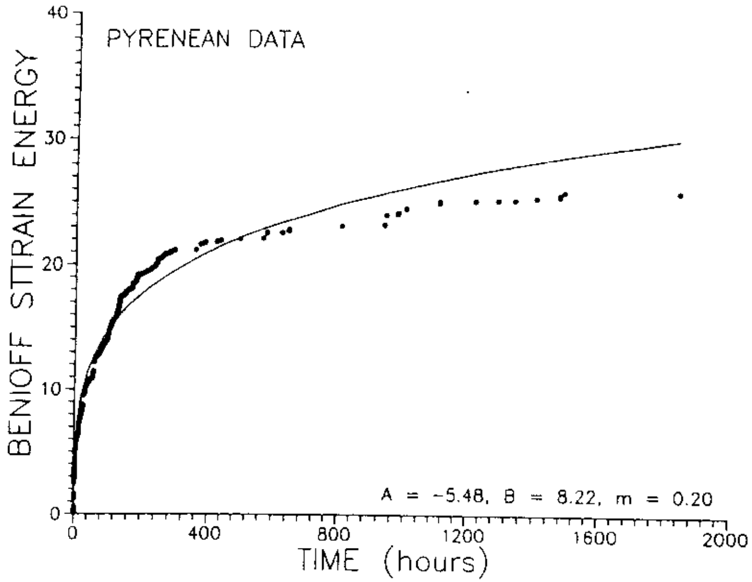
PYRENEAN DATA
BENIOFF STTRAIN ENERGY
A = -5.48, B = 8.22, m = 0.20
TIME (hours)

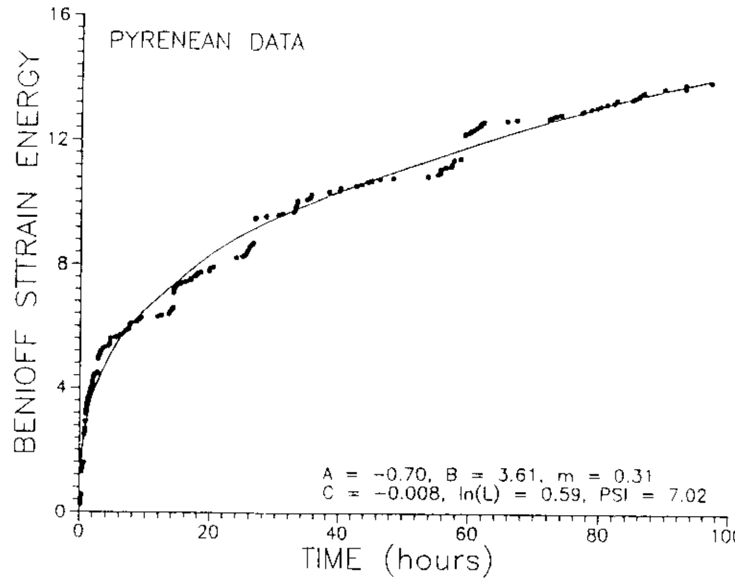
PYRENEAN DATA
BENIOFF STTRAIN ENERGY
A = -0.70, B = 3.61, m = 0.31
C = -0.008, ln(L) = 0.59, PSI = 7.02
TIME (hours)

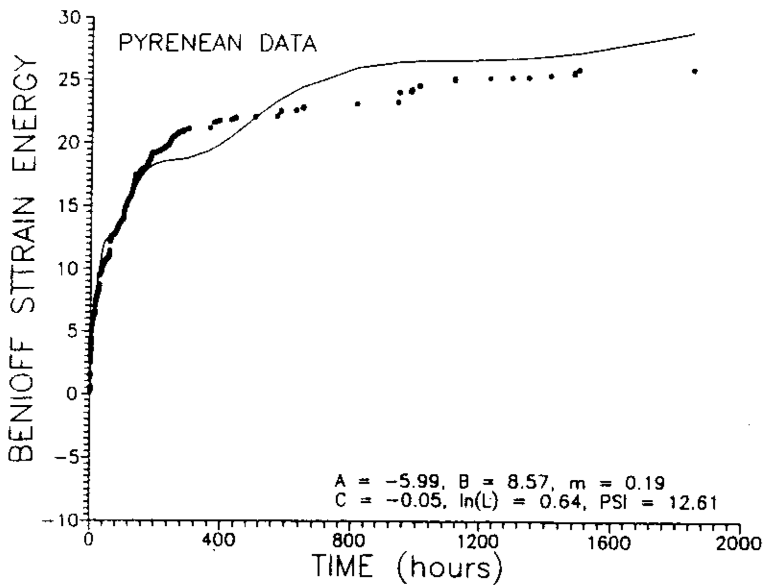
PYRENEAN DATA
BENIOFF STTRAIN ENERGY
A = -5.99, B = 8.57, m = 0.19
C = -0.05, ln(L) = 0.64, PSI = 12.61
TIME (hours)

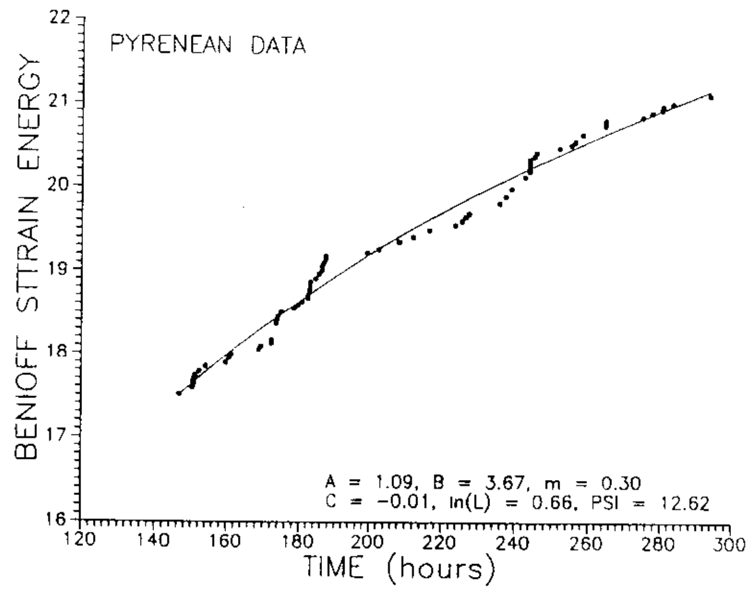
PYRENEAN DATA
BENIOFF STTRAIN ENERGY
A = 1.09, B = 3.67, m = 0.30
C = -0.01, ln(L) = 0.66, PSI = 12.62
TIME (hours)

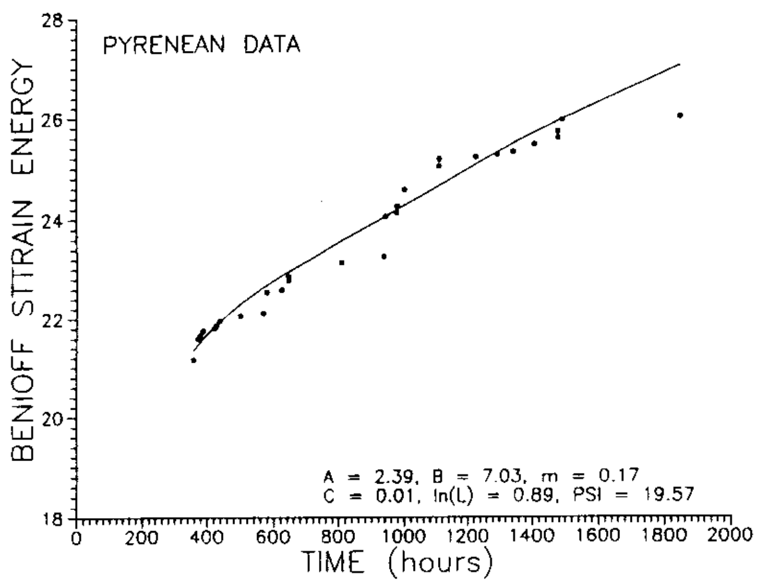
PYRENEAN DATA
BENIOFF STTRAIN ENERGY
TIME (hours)
A = 2.39, B = 7.03, m = 0.17
C = 0.01, ln(L) = 0.89, PSI = 19.57

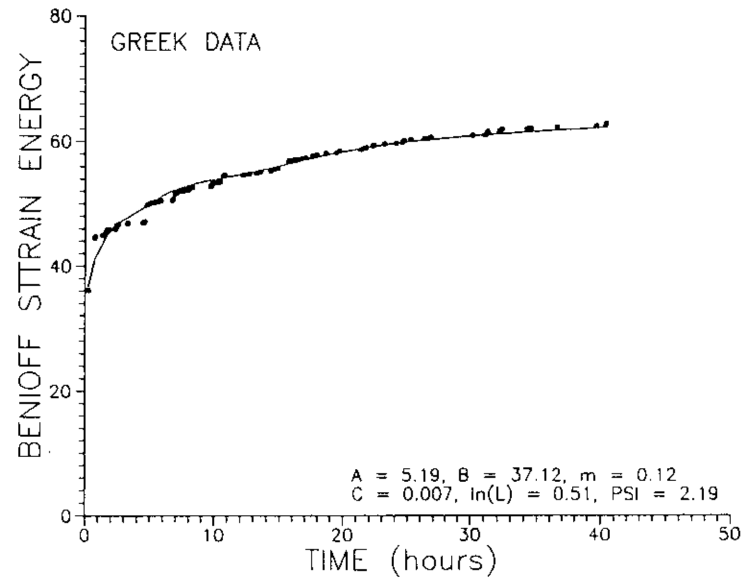
GREEK DATA
BENIOFF STTRAIN ENERGY
TIME (hours)
A = 5.19, B = 37.12, m = 0.12
C = 0.007, ln(L) = 0.51, PSI = 2.19

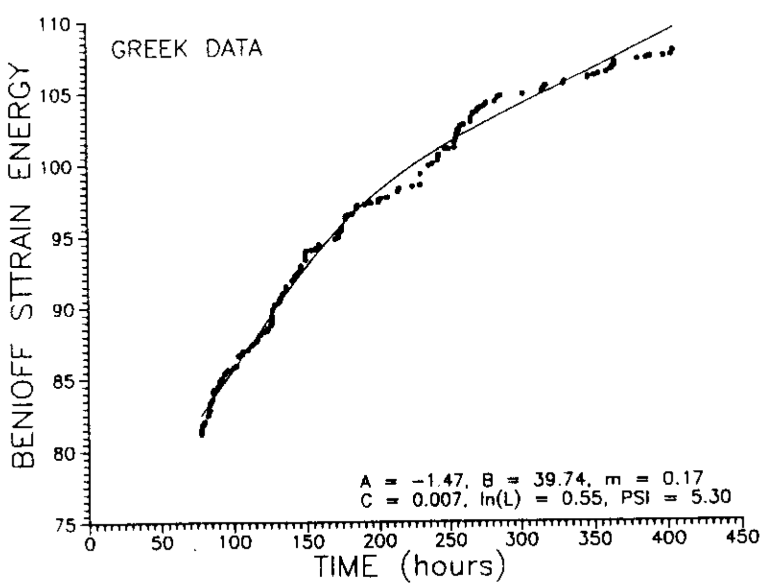
GREEK DATA
BENIOFF STTRAIN ENERGY
TIME (hours)
A = -1.47, B = 39.74, m = 0.17
C = 0.007, ln(L) = 0.55, PSI = 5.30

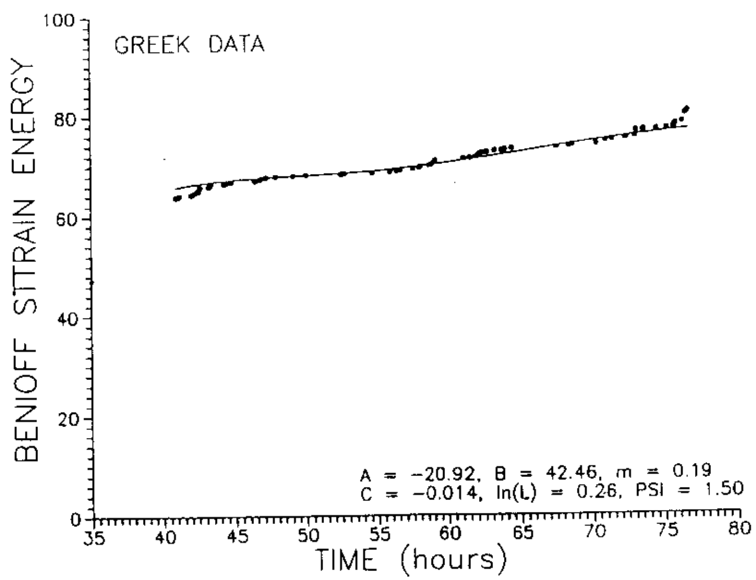
GREEK DATA
BENIOFF STTRAIN ENERGY
TIME (hours)
A = -20.92, B = 42.46, m = 0.19
C = -0.014, ln(L) = 0.26, PSI = 1.50